

**UNCLASSIFIED**

---

---

**AD 276 714**

*Reproduced  
by the*

**ARMED SERVICES TECHNICAL INFORMATION AGENCY  
ARLINGTON HALL STATION  
ARLINGTON 12, VIRGINIA**



---

---

**UNCLASSIFIED**

NOTICE: When government or other drawings, specifications or other data are used for any purpose other than in connection with a definitely related government procurement operation, the U. S. Government thereby incurs no responsibility, nor any obligation whatsoever; and the fact that the Government may have formulated, furnished, or in any way supplied the said drawings, specifications, or other data is not to be regarded by implication or otherwise as in any manner licensing the holder or any other person or corporation, or conveying any rights or permission to manufacture, use or sell any patented invention that may in any way be related thereto.

CATALOGED BY ASTIA 27 671 4  
AS AD NO. \_\_\_\_\_

ASD TDR 62-168

## A REVIEW OF HYPERSONIC FLOW SEPARATION AND CONTROL CHARACTERISTICS

*Louis G. Kaufman, II*  
*Stavros A. Hartofilis*  
*William J. Evans*

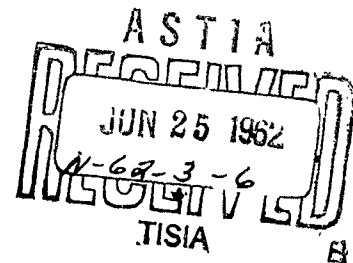
*Richard A. Oman*  
*Lawrence H. Meckler*  
*Daniel Weiss*

GRUMMAN AIRCRAFT ENGINEERING CORPORATION

Contract No. AF 33(616)8130

MARCH 1962

276 714



Flight Control Laboratory  
AERONAUTICAL SYSTEMS DIVISION  
AIR FORCE SYSTEMS COMMAND  
WRIGHT-PATTERSON AIR FORCE BASE, OHIO

## NOTICES

When Government drawings, specifications, or other data are used for any purpose other than in connection with a definitely related Government procurement operation, the United States Government thereby incurs no responsibility nor any obligation whatsoever; and the fact that the Government may have formulated, furnished, or in any way supplied the said drawings, specifications, or other data, is not to be regarded by implication or otherwise as in any manner licensing the holder or any other person or corporation, or conveying any rights or permission to manufacture, use, or sell any patented invention that may in any way be related thereto.

Qualified requesters may obtain copies of this report from the Armed Services Technical Information Agency, (ASTIA), Arlington Hall Station, Arlington 12, Virginia.

This report has been released to the Office of Technical Services, U. S. Department of Commerce, Washington 25, D. C., for sale to the general public.

Copies of ASD Technical Reports and Technical Notes should not be returned to the Aeronautical Systems Division unless return is required by security considerations, contractual obligations, or notice on a specific document.

ASD TDR 62-168

**A REVIEW OF HYPERSONIC FLOW  
SEPARATION AND CONTROL CHARACTERISTICS**

*Louis G. Kaufman, II*  
*Stavros A. Hartofilis*  
*William J. Evans*

*Richard A. Oman*  
*Lawrence H. Meckler*  
*Daniel Weiss*

*GRUMMAN AIRCRAFT ENGINEERING CORPORATION*

*MARCH 1962*

Flight Control Laboratory  
Contract No. AF 33(616)-8130  
Project 8219      Task 821902

AERONAUTICAL SYSTEMS DIVISION  
AIR FORCE SYSTEMS COMMAND  
UNITED STATES AIR FORCE  
WRIGHT-PATTERSON AIR FORCE BASE, OHIO

## FOREWORD

This is the first major report on hypersonic flow separation and control problems which are being investigated by the Research Department of the Grumman Aircraft Engineering Corporation. The work is primarily supported under Contract AF33(616)-8130; Air Force Task 821902. The Project Engineer is Mr. Donald E. Hoak of the Flight Control Laboratory, Aeronautical Systems Division, located at Wright-Patterson Air Force Base, Ohio. Forthcoming reports will present the results of theoretical and experimental research being carried out under the contract.

ABSTRACT

A comprehensive review of high-speed flow separation and a review of available information pertaining to the effectiveness of aerodynamic controls for hypersonic vehicles are presented. Emphasis is on the problems associated with applying the existing information, which relates primarily to the low-supersonic speed range, to hypersonic flow situations. Sufficient detail is presented to allow this report to serve as a self-contained, introductory work on separation phenomena; available sources of specific types of control data are tabulated for ready access.

PUBLICATION REVIEW

This report has been reviewed and is approved.

FOR THE COMMANDER:

*C. B. Westbrook*  
C. B. WESTBROOK

Chief, Aerospace Mechanics Branch  
Flight Control Laboratory

## TABLE OF CONTENTS

<u>Item</u>	<u>Page</u>
Introduction .....	1
Hypersonic Flow Separation .....	3
General Characteristics .....	4
Theoretical Methods .....	8
Crocco-Lees Method .....	10
Other Methods .....	13
Heat Transfer .....	19
Separation on Windward Surfaces .....	20
Incident Shock-Wave Separation .....	21
Steps .....	26
Ramps .....	30
Spikes .....	33
Separation on Leeward Surfaces .....	34
Three-Dimensional and Unsteady Flows .....	37
Flows Over Cavities .....	43
Axisymmetric Bodies .....	48
Experimental Techniques .....	52
Influence of Separation on Controls .....	56
Leading Edge Controls .....	56
Downstream Controls .....	57
Three-Dimensional and Unsteady Flow Effects .....	59
Controls for Hypersonic Vehicles .....	61
General Discussion .....	61
Flaps .....	63
Fins .....	64
Others .....	65
Conclusions and Recommendations .....	67
References .....	70
Appendix - Data Tables .....	96

## LIST OF ILLUSTRATIONS

<u>Figure</u>	<u>Page</u>
1. Characteristics of Separated Flows .....	5
2. Simple Flow Model for Turbulent Boundary Layer Separation .....	14
3. Turbulent Separation Pressure Coefficients .....	16
4. Separation Flow Model Used in Ref. 3 .....	17
5. Boundary Layer Separation by Incident Shock Wave .....	21
6. Incident Shock Surface Pressure Distributions .....	22
7. Separation ahead of a Step .....	26
8. Pressure Coefficient for Turbulent Separation ahead of a Step .....	29
9. Separation ahead of 30° Ramp, $M_\infty \approx 13$ , Grumman Hypersonic Shock Tunnel .....	31
10. Breakaway Separation .....	35
11. Flows over Rearward Facing Steps .....	36
12. Pressure Distribution near Wing-Body Intersection at Hypersonic Speeds .....	40
13. Cavity Flows .....	44
14. Critical Lengths for Cavity Flows .....	46
15. The Laminar White Line .....	54

## LIST OF SYMBOLS

a,b,c	constants in equation on p. 11
A,B	constants in equations on p. 24
$C_{f_0}$	local skin friction coefficient for zero pressure gradient
$C'_f$	local skin friction coefficient due to the (turbulent) Reynolds stress
$C_m$	pitching moment coefficient
$C_p$	pressure coefficient $\equiv \frac{p - p_\infty}{q_\infty}$
F	dependent variable in transformed boundary layer equations
F'	derivative of F with respect to $\eta$
G	function of K and $M_\infty$ defined in equation on p. 15
H	step height
i	enthalpy, steady flow value
i'	enthalpy fluctuation due to flow instability
$\bar{i}$	enthalpy in region of unsteady flow
k	thermal conductivity of air
K	constant in equation on p. 14
L	lift; length of a separated flow region
M	Mach number
n	correlation constant

p	pressure
Pr	Prandtl number
q	dynamic pressure $\equiv \frac{1}{2}\rho V^2$
$\dot{q}$	aerodynamic heating rate
$\dot{q}'$	incremental aerodynamic heating rate due to flow instability
Ra	$Ra \equiv (\text{length of nose spike}) / (\text{maximum diameter of body})$
Re	Reynolds number (based on distance x: $Re_x = \rho u x / \mu$ )
u	velocity component parallel to the surface
$\bar{u}'$	time averaged value of the turbulent fluctuation of the u velocity component
$\bar{u}$	flow velocity along the dividing streamline
$\bar{u}_*$	$\bar{u}_* \equiv \bar{u} / u_\infty$
v	velocity component normal to the surface
$\bar{v}'$	time averaged value of the turbulent fluctuation of the v velocity component
V	resultant velocity $= \sqrt{u^2 + v^2}$
x	distance along the surface measured from the leading edge
y	distance normal to the surface
$\alpha$	angle of attack ~ degrees
$\gamma$	ratio of specific heats
$\delta$	boundary layer thickness
$\delta^*$	boundary layer displacement thickness $= \int_0^\delta (1 - \frac{\rho u}{\rho_e u_e}) dy$

$\delta^{**}$	boundary layer momentum thickness = $\int_0^{\delta} \frac{\rho u}{\rho_e u_e} \left(1 - \frac{u}{u_e}\right) dy$
$\eta$	boundary layer similarity variable
$\kappa$	ratio of mean velocity in boundary layer to the free stream velocity (cf. page 10)
$\mu$	viscosity
$\rho$	density
$\tau$	local shear stress $\equiv \mu \frac{\partial u}{\partial y}$
$\tau'$	local Reynolds shear stress

Subscripts:

aw	adiabatic wall conditions
crit	a critical (or "inspient") condition
e	condition at outer edge of boundary layer
l	laminar boundary layer condition
plat	plateau value
peak	peak value
sep	conditions at the separation point
t	turbulent boundary layer condition
w	conditions at the wall
2	conditions behind shock waves or after reattachment
$\infty$	free Stream conditions

## INTRODUCTION

The problem of hypersonic boundary layer separation is one of extreme importance to the further development of hypersonic vehicles. In the same way that separation leads to sudden changes in flight characteristics which limit performance at lower speeds, it affects the performance limits and allowable design geometries at hypersonic speeds not only by creating undesirable shifts in loads, but also by producing large increases in local heat-transfer rates in reattachment regions, and by creating self-induced oscillations.

Unfortunately, our ability to predict the onset and effects of separation is even more restricted at hypersonic speeds than it is at lower speeds. The nonlinear effects of high Mach number, the large flow property variations within the boundary layer, and the scarcity and questionable accuracy of experimental data contribute to a very limited state of knowledge concerning separation at hypersonic speeds. The well-known difficulties associated with the theoretical analysis of separation problems in general are accentuated at hypersonic speeds by the increased interaction between viscous and nonviscous flows, real gas effects, and the increased relative magnitude of the pressure gradient normal to the surface.

The problem of controlling a hypersonic vehicle is in a similar state of uncertainty. The possible future trend to higher L/D vehicles and the desire to minimize surface area to reduce heat transfer require greater control effectiveness, while non-linearity of the flow, thick boundary layers, strong entropy layers, and three-dimensional flows make aerodynamic control forces more difficult to analyze. The additional problems of separation are so closely connected with control surface design and performance limitations that the study of separation is a necessary prelude to a study of hypersonic control effectiveness.

---

Manuscript released by the authors March 1962 for publication as an ASD Technical Documentary Report.

ASD-TDR-62-168

The purpose of this report is to provide a self-contained description of the present knowledge of problems of hypersonic flow separation and control effectiveness for hypersonic vehicles. We have tried to describe each problem in sufficient detail to provide a working knowledge to the interested reader and to indicate clearly the areas of conflicting opinion and the boundaries of current knowledge. The phenomena which either have been discovered or are expected to occur in special situations are discussed, with particular emphasis on those phenomena which limit performance or constitute a hazard in flight. Although most of the information is digested from the literature, a comprehensive analysis of a considerable amount of it is not available elsewhere. Sources and their content are described clearly, so that those who wish to investigate the field more completely will be able to avoid much of the searching that precedes actual research.

Several recent publications were received too late for review and inclusion in the body of this report. Those containing pertinent and useful information were added to the list of References (Refs. 241 through 252).

## HYPERSONIC FLOW SEPARATION

Comprehensive discussions of various types of separation which can occur in hypersonic flow are presented in this section. The majority of the analyses reviewed treat two-dimensional laminar or turbulent boundary layer separation on either compression or expansion surfaces. Certain aspects of separated flows remain invariant, whereas others change according to the particular mechanism inducing the separation. Our purpose is to present a description of the physical phenomena in the various situations that are important to the aerodynamics and control of hypersonic vehicles, and to discuss available theoretical and empirical methods for treating each problem.

In general, boundary layer separation occurs whenever the streamwise pressure increase along a surface is sufficient to overcome the forces acting to accelerate a fluid particle, or when the streamline curvature necessary to follow the surface contour cannot be sustained by the pressure gradient normal to the surface. In steady-flow aerodynamic problems the only forces acting to accelerate the low-momentum fluid near the wall against a pressure gradient are the shear forces between layers of fluid. Because the momentum of the fluid near the wall is quite low, a relatively small amount of deceleration by the pressure gradient is sufficient to bring about separation. Turbulent flow helps to delay the occurrence of separation, because the turbulent fluctuations increase the effective shear forces and thereby increase the adverse pressure force necessary to reverse the flow of the fluid near the wall.

In high Mach number flows, the pressure loads produced by compression surfaces are much greater than those produced by expansion surfaces. Consequently, the most effective aerodynamic controls usually employ deflections which involve compression of the local flow. Therefore, shock-induced separation, either ahead of a compression surface or due to an incident shock, is the type most prevalent with hypersonic controls and has been studied most extensively.

When separation occurs in high-speed flight, the changes in the pressure distribution and heat-transfer rate can have catastrophic effects. Trim and stability are radically affected by sudden center-of-pressure shifts and changes in pressure magnitude. Local hot spots at separation and reattachment points can cause failure of thermal protection. Heat-transfer rates can also be greatly increased by streamwise vortices originating from three-dimensional

separations.

### General Characteristics

Separated flows are characterized by the prevailing type of boundary layer: laminar, turbulent, or transitional. The pressure rise and the extent of the separated region depend upon the character of the boundary layer. As mentioned previously, the greatly increased effective viscosity due to turbulent fluctuations enables the equilibrium between pressure and shear forces near the wall to occur at much greater adverse pressure rises in turbulent boundary layers. Because of the connection between pressure rise and flow turning angle, this higher pressure corresponds to a much shorter, thicker separated zone for the same initial boundary layer thickness. Cases presented by Schlichting (Ref. 1) and Howarth (Ref. 2) show turbulent pressure rises twice the laminar ones, while the laminar separation zone extends 10 times further than the turbulent one. A similar thickening (and simultaneous pressure rise) occurs in a transitional separation when the mixing zone becomes turbulent, and the downstream flow soon approaches a condition very similar to the equivalent turbulent separation. Upstream of the transition point, the flow has the character of the corresponding laminar separation zone. The location of the transition point therefore plays a distinct role in determining the pressure distribution (cf. Refs. 3 and 4).

Present indications are that shock-induced laminar separation pressure distributions, and to a limited extent turbulent ones, are independent of the type of geometry producing separation (cf. Ref. 3). However, the turbulent peak pressure rise often depends significantly on geometry (Refs. 3 and 5 through 8). This difference in dependence can probably be attributed to the greatly increased effective viscosity in turbulent flow enabling the wall contour within the separated zone to transmit its effect more strongly to the outer flow.

Typical surface pressure distributions are shown in Fig. 1 (cf. Refs. 1 through 4). The laminar boundary layer has a characteristic plateau where the pressure remains almost constant over most of the separated flow region. The separation pressure coefficient is based on the pressure rise from the undisturbed stream to the separation point. As explicitly mentioned by Love (Ref. 9), this is not to be confused with the pressure rise needed to cause separation.

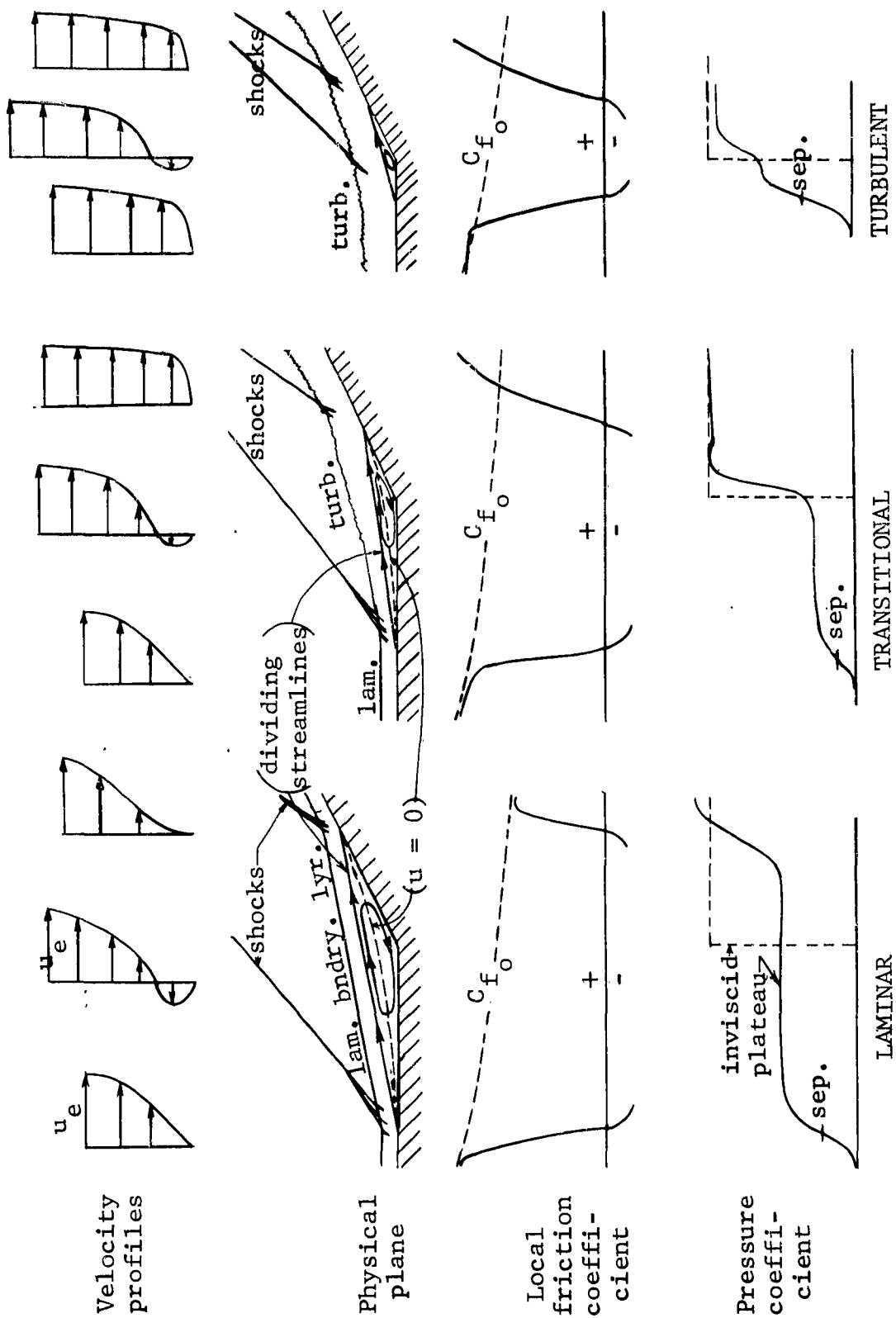


Fig. 1 Characteristics of Separated Flows  
(Examples of Separation ahead of a Ramp)

The separated turbulent boundary layer pressure distribution has no plateau region but rises to a peak value (cf. Refs. 1 and 2). The final pressure after reattachment is usually that given by inviscid theory. Occasionally, a situation arises wherein there is a pressure rise above the inviscid value followed by an expansion to the inviscid value. This is caused by a lower local entropy level due to the multiple-shock compression of the inviscid flow near the separation. The multiple-shock compression is a more efficient process than the single-shock compression, resulting in a higher local total pressure. It has been observed occasionally in three-dimensional hypersonic separation (see Three-Dimensional Effects), and there is good reason to expect it in other situations at high Mach numbers where multiple oblique shock compression can exist.

The critical pressure rise coefficient,  $C_{p_{crit}}$ , sometimes referred to as the incipient pressure rise coefficient, corresponds to the minimum over-all pressure for which separation will occur (cf. Refs. 1, 4, 6, 7, 9 and 10). The current indications are that it is independent of the particular geometry causing the pressure rise (cf. Refs. 8 and 11), although this may not prove to be a completely general rule. As previously discussed,  $C_{p_{crit}}$  is much greater and is a much weaker function of Reynolds number for turbulent boundary layers ( $C_{p_{crit}} \sim Re^{-0.1}$ ) than for laminar ( $C_{p_{crit}} \sim Re^{-0.25}$ ). Correlations are found, however, in earlier works (e.g. Refs. 6, 10, and 12) that give a higher degree of dependence on Reynolds number, but we consider the above exponents closer to the truth in light of the latest theories and experiments.

The pressure rise due to separation (plateau in the case of laminar, peak in the case of turbulent) is of the same order of magnitude as the critical pressure rise, and exhibits the same type of dependence on Mach and Reynolds numbers. In laminar flow the reattachment pressure rise is roughly the same as that of the plateau, but in turbulent flow it is usually from 1/2 to 1/3 of the peak pressure rise. Detailed correlation formulas for predicting the pressure distribution parameters in various situations are given in the later sections.

Two further points should be made concerning the general characteristics of laminar and turbulent separations. First, the increase in Mach number and large changes in stream-to-wall temperature ratio, that are characteristic of hypersonic flow problems,

greatly affect the probability of finding laminar flow at a given Reynolds number, usually in a favorable fashion. And second, the large viscous interaction associated with high Mach number and low Reynolds number will often make it very difficult to determine experimentally or theoretically whether separation has even occurred, let alone the separation location. For those conditions where separation is difficult to detect, the effect of separation on loads is quite small, but the understanding of the flow and the prediction of heat transfer and flow stability becomes uncertain.

The stability and steadiness of separated flows cannot be predicted with certainty using present information. In general, cavities appear to be the most unstable type of separated geometry. Unsteadiness can result from a hysteresis between laminar and turbulent separated-zone conditions if the flow conditions and geometry are of certain types, e.g. a sharply deflected ramp near the transition point of a flat plate. Whether all separated-zone instabilities are associated with transition, or whether other mechanisms participate must be determined by future investigations. The resonant frequency of a cavity would be one important parameter in such an investigation. Violent macroscopic flow fluctuations affect heat-transfer rates and wall shear forces near the separation and reattachment points because of the Reynolds stress effect. This subject is discussed further in the section on Three-Dimensional and Unsteady Flows.

The relationships between heat transfer and separation in laminar and turbulent flow are poorly understood. Chapman (Ref. 13) theoretically estimates a ratio of heat transfer in a laminar separated zone to that in the attached layer, of 0.56 ( see Heat Transfer subsection). The experiments of Larson (Ref. 14) substantiate this estimate. Chapman mentions that turbulent separation regions can have heat-transfer rates as high as six times the equivalent rate for the attached layer at low Mach numbers, but this ratio decreases greatly with increasing Mach number. The turbulent flow measurements of Larson do not show this high ratio at low Mach numbers, but the theory appears to approach the measurements at high Mach numbers. Larson states that the discrepancy is probably due to the failure of the theory to include the proper temperature - heat transfer relationships for the experiments. Current work by Chapman and co-workers supports this view. It appears doubtful whether very large increases in heat transfer will ever be found in steady, separated regions. In short, turbulent and transitional separations may lead to heat-transfer rates higher than the equivalent attached boundary layer, but at high Mach

numbers the ratio appears to be about 0.50 to 0.70, which is not indicated satisfactorily by present theory. Local increases in heat-transfer rate near reattachment are mentioned in Ref. 14, but these were not always found by the other investigators mentioned in Ref. 14.

The converse effect, i.e., the effect of heat-transfer rate on separation characteristics, is also not understood (Refs. 14 through 23). Sogin states in his survey report (Ref. 22) that there is much disagreement between theory and experiment as regards the effects of heat transfer on either laminar or turbulent separated flows. Thus, theoretical results for laminar boundary layers (Refs. 15 through 21) indicate separation should be delayed by cooling; this, however, has not been found experimentally (Refs. 14 and 24 through 26). Gadd further states that if the turbulent boundary layer could be treated analytically it should also show separation delayed by cooling (Refs. 24 and 25), but again, poor experimental agreement is obtained. The resolution of this uncertainty is very important, as it bears directly on the application of wind-tunnel data (equilibrium wall) to flight problems (usually cold wall).

Cooling in the separated region will affect the location of the transition point greatly. Chapman, et al., at NASA Ames Research Center, have unpublished results which show a gradual change from completely turbulent to completely laminar flow in the separated cavity on a blunt, axisymmetric shape. This change was achieved solely by cooling the model. The results of these tests should be published as a NASA report shortly.

### Theoretical Methods

Although many useful methods for predicting boundary layer separation and separated flow characteristics are available, there is as yet no theoretical solution of the problem that results in good quantitative agreement with experimental data. Empirical data and the results of semiempirical methods, where they exist, seem to be the only usable design information. The limited scope of experimental data available, especially for hypersonic problems, and the uncertainties associated with extrapolation can lead to some serious errors in design calculations. The theoretical problem of a separating boundary layer is so difficult that we may

never find a dependable solution without recourse to experimental information. The primary value of present theoretical efforts lies, therefore, in their effect on the treatment and correlation of those data which are available in order to properly generalize the information and accurately determine the limits of applicability.

Theoretical solution to boundary layer flow near separation is complicated by several effects which do not enter the study of attached boundary layer flow. The primary difficulty is associated with the adverse pressure gradient along the surface which in the general case prevents the application of similarity solutions to the boundary layer equations. More basically, we find that the boundary layer equations are often inadequate to describe the flow which occurs near a separation point. This is due to the singular nature of the flow near the separation point and the associated increase in importance of terms in the Navier-Stokes equations which are neglected in the boundary layer equations (e.g., normal pressure gradient and  $\partial^2 u / \partial x^2$ ). We also find that the interaction with the flow outside the boundary layer is different in separated flow, and the external pressure distribution is affected by the behavior of the separated flow. Although these difficulties are sufficient to have prevented solution to low-speed separation problems thus far, there are additional complications in hypersonic flow. The first of these is the hypersonic flow characteristic of nonlinearity between pressure change and local flow angle, requiring a change in the methods commonly used for supersonic flow calculations; the second is the great importance of variations in the transport properties within the separated region which result from the large differences in temperature. In this regard we must expect an increased importance of the wall temperature condition and the heat transfer to or from the separated region on the flow characteristics. Finally, the problem of boundary layer transition and its interaction with the separation phenomena must be considered because of the extremely large change in flow characteristics which accompanies transition in the neighborhood of separated flow. Attempts at the theoretical solution of problems of transition and the behavior of turbulent separated regions are even more primitive than those for laminar flow, but their importance is not diminished in view of the need for basic understanding of the phenomena.

We review current theoretical work on high-speed separation in the following discussion. Because the Crocco-Lees mixing theory (Ref. 27) is the springboard for much of the theoretical work presented in the literature on separation, it is pertinent to begin

this discussion with a brief introduction to it. Applications of the Crocco-Lees method to the problem of separation are discussed, followed by a discussion of other theoretical approaches.

### Crocco-Lees Method

Basically, the Crocco-Lees method (Ref. 27) is an approximate integral method which uses correlation techniques. Previous integral methods, such as the Karman-Pohlhausen method (Ref. 1, p. 206), relate a single parameter, which describes the shape of the velocity profile in the boundary layer, to the local external-stream velocity gradient. These methods are inadequate for separated flows. For example, the Karman-Pohlhausen method fails for large positive pressure gradients such as those associated with separation. Thwaites' method (Ref. 28), which correlates boundary layer profiles and local pressure gradients, yields a Blasius flat-plate profile for zero pressure gradient and so fails in the separated laminar plateau region. Nevertheless, modifications of these theories are being sought to make this type of approach applicable to separated boundary layers (cf. Ref. 29).

Crocco and Lees introduced a new boundary-layer parameter which is a nondimensional ratio of the mean velocity in the boundary layer to the free-stream velocity. This parameter,  $\kappa$ , can be shown to be a function of the boundary-layer thickness,  $\delta$ , the displacement thickness,  $\delta^*$ , and the momentum thickness,  $\delta^{**}$ , as follows:

$$\kappa = \frac{\delta - \delta^* - \delta^{**}}{\delta - \delta^*}$$

In terms of this parameter a friction correlation function, a mixing-rate correlation function, and a mean-temperature correlation function are obtained from known boundary-layer solutions or from experiment. In their original paper, Crocco and Lees obtained these functions from incompressible Falkner-Skan solutions (Ref. 1, p. 118). More recent works (Ref. 30 and 31) have used other boundary-layer solutions, or empirical correlations.

These functions are used in the momentum integral equation and in a second integral equation which is a continuity relation expressing the rate of mixing of fluid from the external region

(isentropic stream) with that of the internal region (boundary layer or dissipative-flow region). Crocco and Lees consider that this mixing process is the fundamental mechanism in the growth of a boundary layer.

The correlation functions that are obtained from similarity solutions of the incompressible boundary layer are related to an entire family of compressible flows through the Stewartson transformation (cf. Ref. 32). Although the arbitrariness in defining the boundary layer thickness would seem to lead to great uncertainties because the value of  $\kappa$  is seen to be sensitive to the value of  $\delta$ , Gadd and Holder (Ref. 25) and Glick (Ref. 31) show that results of the method are fairly insensitive to any conventional choices of  $\delta$ . The Crocco-Lees method is limited to the case of zero heat transfer at the wall, constant stagnation enthalpy, small flow deflection angles, and the standard boundary layer assumption that the static pressure gradient normal to the wall is negligible within the boundary layer. Crocco and Lees apply their method to the problem of determining base pressure and various other problems in their report (Ref. 27).

Cheng and Bray (Ref. 30), apply the Crocco-Lees method to the separation produced by the interaction between an incident shock wave and a boundary layer over a flat plate, as suggested by Crocco in Ref. 33. They are unsuccessful in finding suitable correlation functions for other than laminar flow, and even for laminar flow, the results of the final calculations agree only qualitatively with experiment. The calculated length of the separation bubble, for example, is an order of magnitude larger than that observed experimentally.

In a follow-on investigation by Cheng and Chang (Ref. 34), the application of the Crocco-Lees method is restricted to a completely laminar boundary layer. The aim was to determine the minimum shock strength required to produce separation in a laminar boundary layer. The calculated results are presented by means of a simple formula which may be written as

$$C_p = \frac{p - p_\infty}{\frac{\gamma}{2} M_\infty^2 p_\infty} = \frac{a (M_\infty - b)}{\frac{\gamma}{2} M_\infty^2} (Re_s \times 10^{-6})^{-c}$$

where  $Re_s$  is the Reynolds number based on the distance from the leading edge to the separation point.

In the case of  $C_{p_{sep}}$  the calculated results show that  $a = 0.081$ ,  $b = 0.4$ , and  $c = 0.160$ . In the case of  $C_{p_{crit}}$   $a = 0.060$ ,  $b = 0.5$ , and  $c = 0.186$ . These formulas would agree with the available experimental data of Ref. 3 if for  $C_{p_{sep}}$  the value of "a" were equal to 0.040. The same would be true for the data of Ref. 35 if for  $C_{p_{sep}}$ , "a" were equal to 0.056, and for  $C_{p_{crit}}$  "a" were equal to 0.120. These results indicate good qualitative agreement with experiment but unsatisfactory quantitative agreement. The authors claim, however, that the quantitative difference is not as great as the differences among the experimental data insofar as pressure ratio is concerned.

Glick, (Ref. 31), uses the theoretical studies of Thwaites, Howarth, Falkner-Skan, and Hartree, (Refs. 28, 36, 1, p. 118, and 37) and the experimental study of flow over an ellipse by Schubauer (Ref. 38) in an attempt to find relations for the Crocco-Lees correlation functions in terms of  $\kappa$ , for the flow region up to the separation point. Beyond the separation point, the correlation functions are obtained by means of experimental data. The conditions of the experiment selected are  $M_\infty = 2.45$  and  $Re_\infty/\text{inch} = 6 \times 10^4$ . The technique is employed in the reattaching region as well, using data from the same experiment. Glick claims to have achieved quantitative success with this approach. However, in the region downstream of separation the correlation functions are obtained from experimental conditions that are close to the conditions that the calculated results are compared with; caution is advisable here. His calculations are for the case of separation induced by a shock wave interacting with a laminar boundary layer in a free stream of Mach 2, and a separation Reynolds number of  $2.3 \times 10^5$ . He has also completed calculations for a case where the Mach number is 5.8 and the separation Reynolds number is  $1 \times 10^5$ , but unfortunately, no experimental data were available to check these results. Glick explains why previous uses of Falkner-Skan solutions to obtain the correlation functions have not resulted in good correlation with experiment. The basic reason is "the physical fact that Falkner-Skan flows are similar flows which do not have histories and do not reflect the essential change in shape of the velocity profile prior to separation."

Based on the results that Glick has had with his modification of the Crocco-Lees method, he appears to be very optimistic concerning its further use. He suggests that more calculations be

made with this method for other separated flow geometries such as forward and rearward facing steps, corners, cutouts, ramps, etc. As noted above, Glick maintains that the method is not sensitive to the definition of the thickness of the boundary layer.

Bray, Gadd, and Woodger (Ref. 39) obtain their relations for the Crocco-Lees correlation functions from the similarity solutions of the compressible, laminar boundary layer by Cohen and Reshotko, (Refs. 15 and 16). The relations are derived and presented in terms of the velocity ratio  $F'$ , and the similarity variable,  $\eta$ . Some of these similarity solutions have negative values of  $F'$  at low values of  $\eta$ , indicating reverse flow near the wall. These are called "lower-branch" solutions and were first discovered and named by Stewartson (Ref. 40).

Prior to the approach of Bray, Gadd, and Woodger it was assumed that the boundary layer was bounded at its inner edge (in the separated zone) by a region of relatively motionless flow. The approach taken in Ref. 39, (or Ref. 25), was to base the relations for the Crocco-Lees correlation functions on the lower-branch solutions of Cohen and Reshotko in the separated zone, as mentioned above, and on the upper-branch solutions for the attached region of flow. This approach is more in keeping with the experimental observation of flow reversal near the wall after the separation point. Nevertheless, the authors claim that the results of this approach agree only qualitatively with experiment. Because of this and because of the algebraic complexity of the method, they suggest the use of a new and simpler method which they present. This new method is a Pohlhausen-type method and does not result in better agreement with experiment, although the results are as good as those of the Crocco-Lees method. An important result of their calculations, however, is the discovery of the "laminar foot" (cf. Fig. 1, page 5) which had not been shown in previous analyses of separated laminar boundary layers.

#### Other Methods

Hammit (Ref. 5), using a simple flow model for turbulent boundary layer separation due to an abrupt increase in pressure (Fig. 2), postulates that within the small shock-wave boundary-layer interaction region the transport of mass and momentum into

the boundary layer is small. Also, near separation, shear forces at the wall are neglected in the shock-wave boundary-layer interaction region. Conservation of mass and momentum are used to connect the upstream and downstream equilibrium boundary layers adjusted through the small interaction region where the pressure changes are large. Mass and momentum transfer from either the stream or the wall and the effect of skin friction are neglected in this region. A one-parameter boundary layer profile is used and only average conditions through the boundary layer are considered; a parameter is defined as the ratio of an average velocity to the velocity at the edge of the boundary layer, the average velocity being taken as the ratio of the momentum to the mass flow.

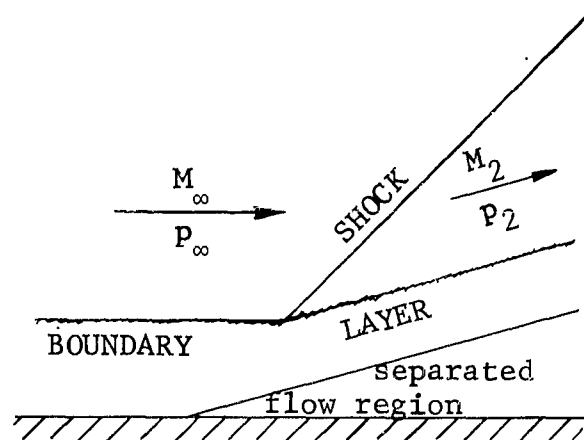


Fig. 2 - Simple Flow Model for Turbulent Boundary Layer Separation

Hammitt is one of many who express the opinion that the effects of compressibility on boundary layers should be of a quantitative rather than a qualitative nature (cf. Refs. 5 and 11). Schuh (Ref. 11), Mager (Refs. 41 through 43), and Culick and Hill (Ref. 44) present transformations used in extending incompressible solutions to compressible flow cases. Mager obtains an incompressible relationship between the velocities immediately upstream and downstream of separation,  $V_2^2 = KV_\infty^2$ , and similarly relates the corresponding Mach numbers across shock waves for compressible flows  $M_2^2 = KM_\infty^2$  (see Fig. 2). The experimental range of  $K$  is between 0.49 and 0.60 regardless of the geometric mechanism causing separation. Using Schuh's empirical results, Mager (Ref. 42) arrives at the following expressions for the pressure ratios for turbulent separation:

$$\frac{P_{\text{sep}}}{P_\infty} = 1 + \frac{\gamma}{2} M_\infty^2 \left[ \frac{1 - K}{1 + \frac{\gamma-1}{2} M_\infty^2} \right]$$

and

$$\frac{P_2}{P_\infty} = \frac{P_{sep}}{P_\infty} \left[ \frac{1 + G}{1 + G \frac{P_{sep}}{P_\infty}} \right]$$

where

$$G = -0.328 \frac{K \sqrt{M_\infty^2 - 1}}{1 + \frac{\gamma - 1}{2} K M_\infty^2}$$

and

$$K = 0.55$$

Separation and final pressure coefficients, obtained from the above empirical theories and experimental correlations, are plotted in Fig. 3 (cf. Refs. 5, 11, 43, and 45). The results all agree fairly well with Schuh's experimental correlation.

It is important to remember, however, that a certain amount of agreement is guaranteed in each case by the use of empirical data in evaluating constants and parameters for the different theories. This is especially important when we consider their extension to higher Mach numbers. The flow model used in Ref. 5 indicates a decrease in the thickness of the turbulent boundary layer whereas all other theoretical and experimental evidence indicates that the boundary layer will thicken downstream of the shock-wave

boundary-layer interaction region (see, e.g., Ref. 2, p. 472).

Bogdonoff and Kepler (Ref. 46) study turbulent boundary layer interaction using a flow model which they feel susceptible to the type of treatment proposed by Crocco and Lees; they point out, however, that more information on mixing rates, particularly in the separated flow region, is needed for the direct application of the Crocco-Lees method. In a more recent work, Gadd (Ref. 47) presents a simple new method for treating the interaction of normal shock waves and turbulent boundary layers on flat surfaces.

The problem of separation for both turbulent and laminar compressible boundary layers is treated by Honda (cf. Refs. 48 and 49). He splits the turbulent boundary layer into an outer, essentially inviscid, layer and an adjacent, inner, viscous layer. For the laminar layer prior to the point of separation, Honda uses the momentum integral equation, the energy integral equation, and the mixing rate continuity equation. He introduces four parameters after applying Stewartson's transformation and determines the relations between them by using Pohlhausen's fourth degree polynomial for the velocity profile. For the laminar separated layer, he assumes a physical model in which the separation streamline represents the "wall" of the layer where  $u = 0$ . He assumes that the usual boundary layer assumptions still hold in the separated layer and transforms the mass, momentum, and energy flux equations again using Stewartson's transformation. He then makes two assumptions: that the separation streamline is a straight line, and that the boundary layer profile in the layer is similar to the profile at the point of separation. The results of this approach upstream and immediately downstream of the point of separation agree reasonably well with experiment for  $M_\infty \approx 2$  to 3.

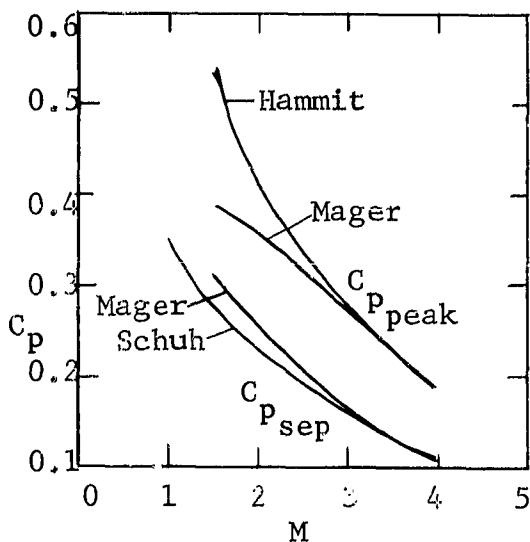


Fig. 3 - Turbulent Separation Pressure Coefficients

Semiempirical theories for laminar separation, based on simpler flow models than that used in the Crocco-Lees method, have been proposed by Gadd (Refs. 50 and 51), Chapman (Ref. 3), Donaldson (Ref. 12), and others. Pressure distributions are considered first in the absence of heat-transfer effects.

The general qualitative shape of the pressure distribution curve in the region of incipient separation of laminar boundary layers is presented in an early paper by Gadd (Ref. 50); the actual separation point cannot be determined because the boundary layer is represented by similar profiles (Refs. 15 and 16) and so the separation profile is never realized. A more quantitative approach taken by Gadd (Ref. 51) is to split the boundary layer into two adjacent layers: a very thin layer next to the wall and an outer layer comprising the remainder of the boundary layer. The outer layer may be calculated using an essentially inviscid analysis. The inner layer is calculated by requiring that the shear and pressure gradients balance and that the profile of the inner layer smoothly join that of the outer layer. The line separating the layers is not necessarily a streamline. Gadd accomplishes this for the general case and then for the simpler case when the inner layer may be assumed to be only a minor portion of the total thickness of the boundary layer. The differences in the results are almost nil. In this manner the  $C_{p_{sep}}$  equation on page 24 is obtained. A similar procedure, but using several adjacent layers, is currently proposed by C. Donaldson of A.R.A.P. A theoretical treatment of moderately separated flows due to a prescribed, continuous, (isentropic) pressure rise is presented by Bloom in Ref. 67. The velocity profile is assumed representable by a fourth degree polynomial and the integral method, described on pages 206 and 289 of Ref. 1, is used.

Leading edge separation and reattachment are analyzed by Chapman, Kuehn, and Larson (Ref. 3). Their flow model is shown in Fig. 4. A uniform

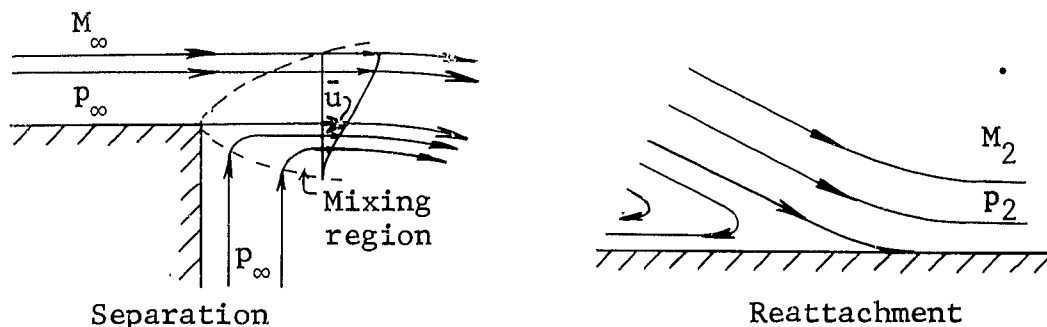


Fig. 4 - Separation Flow Model Used in Ref. 3

stream with no boundary layer, mixes with a dead air region of equal pressure. The mixing region grows parabolically, similar to the growth of laminar boundary layers, and is composed of similar profiles. Therefore, the velocity ratio  $\bar{u}/u_\infty$ , where  $\bar{u}$  is the velocity along the dividing streamline, remains constant. The Blasius equation may then be solved and, for a linear viscosity-temperature law, it is found that the velocity ratio is constant:  $\bar{u}/u_\infty = \bar{u}_* = 0.587$ . Furthermore, for Mach numbers less than 5 and a power law relationship between viscosity and temperature, the value of  $\bar{u}_*$  is essentially constant; thus, regardless of Reynolds number, streamwise station, viscosity-temperature law, and Mach number,  $\bar{u}_* \approx 0.587$  as long as the initial velocity is uniform. The dividing streamline at separation, by continuity for steady flows, must be the dividing streamline at reattachment. The mass flow scavenged from the dead air region by the mixing layer must equal the mass flow reversed back into the dead air region by the pressure rise at separation. Assuming isentropic compression of the stream flow at reattachment, Chapman, Kuehn, and Larson (Ref. 3) obtain the expressions

$$\frac{p_\infty}{p_2} = \left[ \frac{1 + \frac{\gamma-1}{2} M_2^2}{1 + \frac{\gamma-1}{2} \frac{M_2^2}{(1 - \bar{u}_*^2)}} \right]^{\frac{\gamma}{\gamma-1}}$$

and

$$M_2^2 = (1 - \bar{u}_*^2) M_\infty^2 \quad \text{for} \quad \bar{u}_* = 0.587, \quad M_2^2 = 0.655 M_\infty^2$$

where subscript  $\infty$  indicates undisturbed stream conditions and subscript 2 indicates conditions at the end of the reattachment zone. Thus, the pressure rise across reattachment is given in the first

equation and, from the second equation and using  $\bar{u}_* = 0.587$ , the Mach number ratio across reattachment. The second equation is of the same form as Mager's equation on page 15 but the constant for the isentropic pressure rise at reattachment is higher.

#### Heat Transfer

Chapman, Gadd, and several others present analyses including heat-transfer effects (cf. Refs. 13 through 24 and 51). Chapman (Ref. 13) uses the same flow model as shown in Fig. 4 and a compressible-flow modification of the von Mises stream function transformation (Ref. 1, page 122). The momentum and energy equations are solved for the case of constant wall enthalpy for various values of the Prandtl number, and Sutherland's viscosity-temperature law (Ref. 53, page 168). The velocity ratio along the dividing streamline is again found to be constant and equal to 0.587, and variations of  $Pr$  were found to affect the results negligibly. Boundary-layer theory is again assumed to be valid in the mixing region. Chapman's results are only for the over-all heat transfer to the separated flow region and do not represent a heat-transfer distribution. He obtains the results that the average heat-transfer rate for a separated laminar boundary layer is 56% of the heat-transfer rate for an attached laminar boundary layer on a flat plate. Chapman (Ref. 13) presents the low Mach number turbulent separated case for  $Pr = 1$  and obtains the result that the average heat transfer in a turbulent separated region may be 6.3 times as great as that for an attached turbulent boundary layer on a flat plate. Considerable doubt exists as to the accuracy of this result, as it is not evident in experiments (see General Characteristics). He also calculates the effective skin friction in the separated laminar case and finds it to be about six tenths of the attached value. The case of fluid injection into the dead air region is considered, and it is shown that minor mass injection would greatly reduce the heat transfer to the wall.

Gadd (Ref. 51) states that his theory, as described above, predicts that cooling a wall increases the pressure rise required to separate a laminar boundary layer. In agreement with Gadd, Poots (Ref. 54) shows that heating a wall encourages separation. Gadd states that although his results may be qualitatively correct, they are useless quantitatively and that the unrigorous dimensional arguments presented by Chapman (Ref. 13) give much better agreement for

over-all heat transfer with the experimental work of Larson (Ref. 14). Heat transfer effects on separated flow regions were investigated using observations of free flight tests at supersonic (Ref. 52) and at hypersonic (Ref. 65) Mach numbers. Lankford presents experimental data which demonstrate that laminar separation ahead of axisymmetric compression corners is delayed by reducing the wall temperature. The extent of separation is reduced and the inviscid pressure distribution is approached as the wall temperature is lowered, whereas heating the wall causes upstream movement of the separation point (Ref. 65).

Experimental evidence obtained by Larson (Ref. 14) and also by Seban, Emery, and Levy (Ref. 55) for separated turbulent boundary layer flows indicate the failure of theoretical analyses in predicting the heat-transfer effects. For example, the theory postulated by Chapman (Ref. 13) described above, does not give reasonable estimates for even the over-all, (average) heat transfer, much less the detailed distribution of heat transfer, to regions for separated turbulent boundary layers. Further work on heat-transfer effects on separated-zone pressures and transition is currently in progress at NASA, Ames Laboratory. The dearth of papers on theoretical and experimental research on heat-transfer effects for separated turbulent boundary layers is brought out in several survey type reports (cf. Refs. 22 and 56).

Finally, Kuo (Ref. 23) determined that although dissociation does greatly reduce the thermal boundary layer thickness and lowers the temperature at the outer edge of the boundary layer, the inclusion of dissociation effects for a gas in dissociated equilibrium does not affect either the heat flux or the friction coefficient at the wall for either laminar or turbulent boundary layers. Dissociation effects may be included in boundary layer analyses by using Cohen's correlation formulas and tables (Ref. 57).

### Separation on Windward Surfaces

The major portion of the forces acting on a hypersonic vehicle are experienced by the compression surfaces, and the understanding of the flow field over such surfaces is of paramount importance. Shock induced separation, due to incident shock waves, forward facing steps, ramps and spikes, is treated here. Except for a single study of separation due to supersonic isentropic compression (a filleted ramp), virtually all studies that we describe involve shock-wave boundary-layer interaction.

## Incident Shock-Wave Separation

A boundary layer may separate locally because of the pressure rise associated with a shock wave generated by an external body and incident to the boundary layer, as sketched in Fig. 5 (from Howarth, Ref. 2, page 472.) In flight the shock generator may be a fin, or perhaps the lip of an intake (Refs. 6 and 58). In an experiment the shock generators are usually placed parallel to the surface being studied; a wedge may be used to generate a two-dimensional shock incident to the boundary layer on a wind-tunnel wall or on a model in the tunnel.

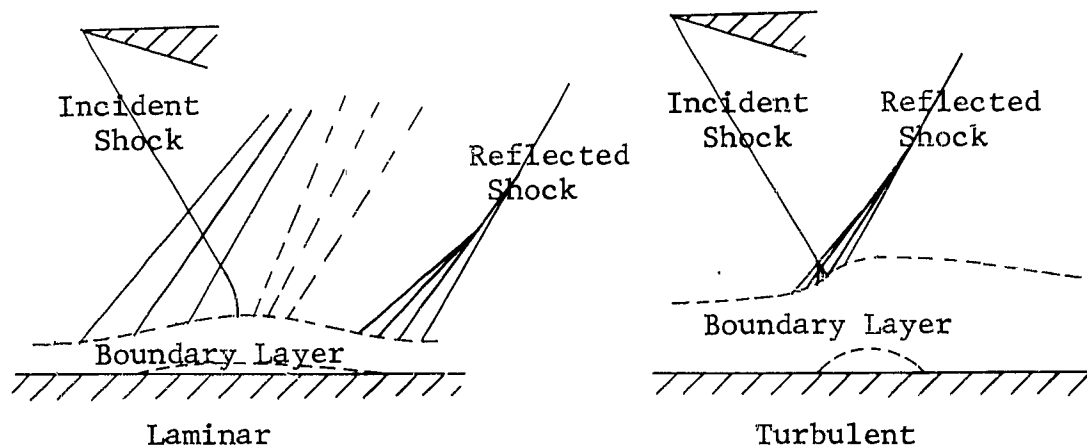


Fig. 5 Boundary Layer Separation  
by Incident Shock Wave

The study of separation is somewhat simplified when the pressure rise is due to a shock wave generated by an external object. The location of the inviscid shock wave is not affected by the interaction. Also, the approximate location of the separated flow region may be determined from the undisturbed boundary layer thickness and the location of the inviscid shock. One complicating factor, on the other hand, is the existence of both incident and reflected shocks. As in all separation problems, the classical boundary layer simplifications are no longer valid near the interaction zone. In this connection, Bogdonoff and Kepler (Ref. 46) have shown experimentally that the normal pressure gradients,  $\partial p/\partial y$ , can be as high as twice the value of the streamwise gradients,  $\partial p/\partial x$ , just before the separation point.

Laminar boundary layers cannot withstand pressure gradients as high as turbulent ones can. The inviscid pressure rise is

spread over a larger surface distance because the laminar shear stresses are less than the turbulent. This is evidenced in Fig. 6, which shows surface pressure distributions for incident shocks on laminar and turbulent boundary layers. The Mach number

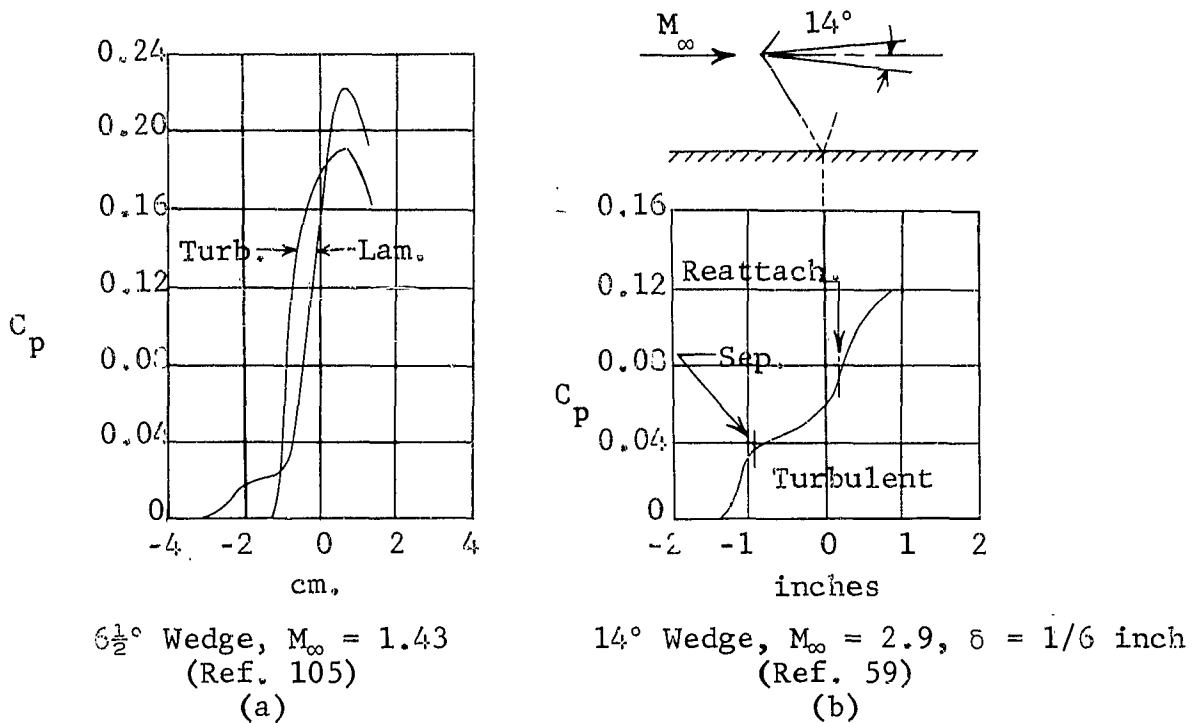


Fig. 6 Incident Shock Surface Pressure Distributions

was 1.43, the undisturbed laminar boundary layer thickness was about 0.7 mm, and the corresponding turbulent boundary layer thickness was about 1.4 mm. The length of diffusion was equal to about  $100 \delta_l$  in the case of interaction with a laminar boundary layer, decreased to about  $10 \delta_t$  for a turbulent boundary layer; the symbol  $\delta$  denotes boundary layer thickness in the shock region.

Vas (Ref. 59), Bogdonoff and Kepler (Ref. 46), and Vas and Bogdonoff (Ref. 60), present several surface pressure distributions for turbulent boundary layer separation caused by incident oblique shocks. A sample of their data is shown in Fig. 6 for a wedge semi-vertex angle of 14° and a free stream Mach number of 2.9. The

points of separation and reattachment are indicated. The separated flow region was about  $(3/4) \delta_t$  in height and  $6\frac{1}{2} \delta_t$  long, where  $\delta_t$  is the thickness of the undisturbed turbulent boundary layer. Vas states that the boundary layer for the case presented in Fig. 6b was "definitely turbulent". The greater spread of the pressure rise, over that shown in Fig. 6a for a turbulent boundary layer, is due to the much smaller shock angle and thicker boundary layer. The wedge angle was varied from 8 to 14 degrees and total pressure probes, both forward and rearward facing, were used to survey the entire interaction region. The boundary layer did not separate for the 8° wedge; for all greater wedge angles the boundary layer did separate, with the length of the separated flow region increasing with wedge angle. The streamwise Mach number distribution, measured 0.01" above the wall, was plotted versus  $x$  for all wedge angles. For the 8° wedge there is a large dip in the curve and separation is nearly incipient. For the thicker wedges the dip goes below the  $M = 0$  axis, indicating reverse flow. The plots are similar in shape to the local friction plots shown in Fig. 1, page 5. The pressure ratio across the 8° wedge shock of Vas, for  $M_\infty = 2.9$ , is just less than 1.8 (Ref. 61). This pressure ratio is equal to that needed to separate a turbulent boundary layer by a normal shock wave (Ref. 1). It appears from this that the critical pressure rise is relatively insensitive to the geometry of the incident shock wave, but is a function of the strength of the shock wave.

Investigations of pressure rises associated with turbulent boundary layer separation caused by incident shocks (sometimes referred to as reflected-shock separation) are presented in Refs. 3, 6, 7, 9, 41, 42, 43, 46, 59, and 62. In Fig. 43 of the report by Chapman, Kuehn and Larson (Ref. 3), the separation pressure rise for incident shocks is plotted versus Reynolds number for three Mach numbers. The separation pressure rise for turbulent layers is a weak function of Reynolds number, becoming essentially independent of Reynolds number as the free stream Mach number increases and, in agreement with Schuh (Ref. 11), as the Reynolds number increases over about  $10^7$ . As mentioned earlier, Mager (Refs. 41 through 43) obtains separation pressure rises which are independent of geometry; thus, the theoretical relations presented on page 14 are taken to hold for incident shocks.

Shock waves incident to laminar boundary layers have been studied by Hakkinen et al., Gadd, and Greber (Refs. 18, 35, 51, and 63) and are discussed in the works of Lange and Love (Refs. 6 and 9).

From the various theoretical and experimental works, the following two equations are obtained for the laminar separation pressure rise and the laminar plateau, respectively

$$C_{P_{sep}} = A \left[ Re_x (M_\infty^2 - 1) \right]^{-\frac{1}{4}}$$

$$C_{P_{plat}} = B \left[ Re_x (M_\infty^2 - 1) \right]^{-\frac{1}{4}}$$

The coefficients A and B are defined in the following table where pertinent remarks are also made. These equations are derived by relating  $C_{P_{sep}}$  and  $C_{P_{plat}}$  to the skin friction coefficient which would exist at the separation point if the pressure were constant.

TABLE 1  
CONSTANTS IN CORRELATIONS OF SEPARATION PRESSURES

Ref. No.	Author	$M_\infty$ Range	A	B	Remarks
51	Gadd	$M_\infty > 1$	1.13	-	Theoretical; thickness of inner profile assumed small
3	Chapman	$1 < M_\infty \leq 3.6$	.93	1.82	Empirical fit*
35	Hakkinen	$M_\infty \approx 2$	1.15	1.90	Theoretical estimate; satisfactory correlation for $M = 2$ only

\* Presented in Refs. 51 and 4, obtained from data of Ref. 3.

Since present indications are that the laminar separation pressure rise and laminar plateau pressure are independent of the type of shock inducing separation, the above equations hold as well for other types of laminar separation. As new results are obtained, however, the form of the equations, and the values of the coefficients A and B, may show dependence on geometry as the Mach number increases.

Hakkinen, et al., (Ref. 35) derive a relationship for the plateau pressure rise, namely

$$C_{P_{\text{plat}}} = 1.65 C_{P_{\text{sep}}}$$

This expression agrees quite well with the data at  $M_{\infty} = 2$ ; at other Mach numbers its validity has not been verified. They further note that the boundary layer profiles are modified near the wall in the separated flow region. Outside of the reverse-flow region the boundary layer behaves much as an undisturbed boundary layer. Upstream and downstream of separation for the laminar case the skin friction is close to the Blasius value. If the separated flow region is long enough, the characteristic laminar plateau appears. The pressure rises to the plateau value from its undisturbed value upstream of separation and then rises to the final pressure downstream of reattachment; the final pressure corresponds to that behind the incident and the reflected shock waves. Their theoretical treatment is based on these experimental observations.

Two-dimensional surface curvature effects on the pressure rises associated with oblique shock waves incident to laminar boundary layers are presented by Greber and Gadd (Refs. 18, 51, and 63). Experimental results indicate that the curvature effects can merely be superimposed on the flat plate interaction results. Curvature leads to a favorable pressure gradient flow which is calculable using Prandtl-Meyer expansion. Thus, the strength of the incident shock causing incipient separation must be increased to account for the Prandtl-Meyer decrease in pressure, the critical pressure coefficient remaining unchanged. So also, for separated boundary layers, the pressure in the separated region, the plateau pressure, is reduced on the curved wall by the inviscid pressure decrease associated with the curvature.

The boundary layer may be laminar at separation and become turbulent before reattachment; separation of this transitional

type of boundary layer by incident shock waves exhibits the general characteristics discussed earlier. The laminar plateau region is shortened, and downstream of transition the pressure distribution is similar to that for turbulent boundary layers (cf. Fig. 1 of this report, Fig. 18 of Ref. 3). Hakkinen's (Ref. 35) results indicate a large increase in skin friction for turbulent reattachment; also, the pressure usually rises above its inviscid value and must decay back down to it whereas, for laminar reattachment, the pressure rises monotonically to its inviscid value.

### Steps

Boundary layer separation is to be expected ahead of forward-facing steps as long as the step height is not negligible in comparison to the thickness of the boundary layer. Thus, even small ridges on a surface may cause separation and alter the pressure distribution, particularly so for turbulent boundary layers. Sketches of such flows and typical pressure distributions

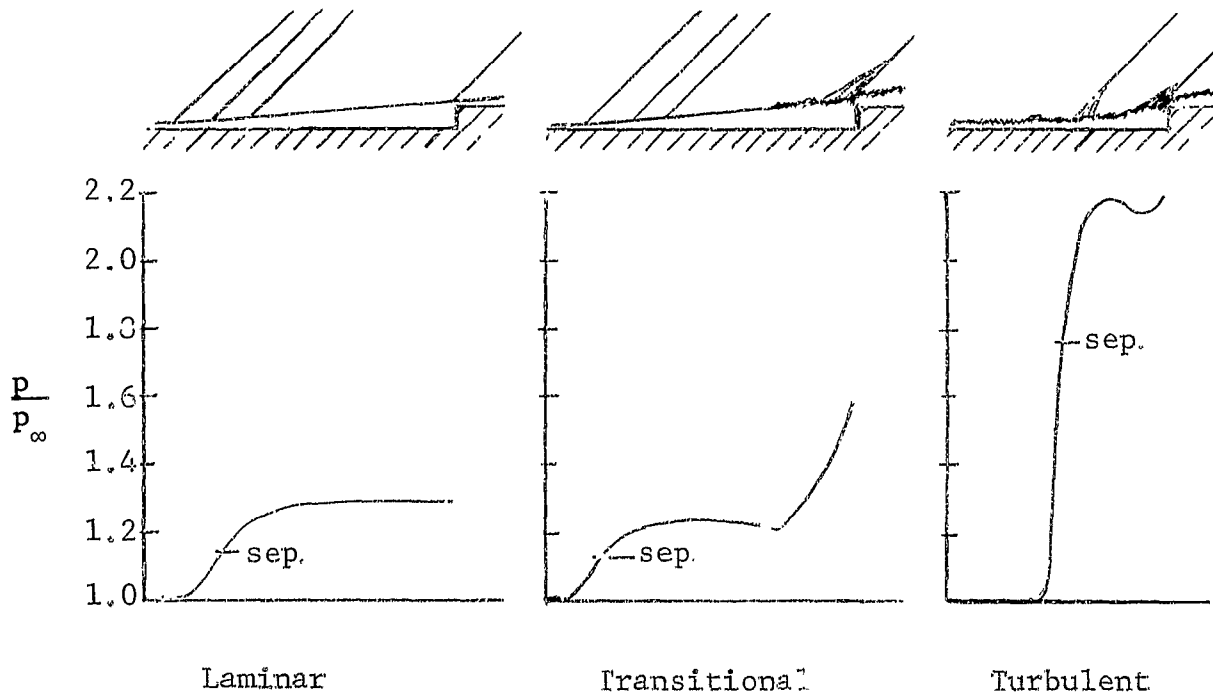


Fig. 7 Separation ahead of a Step  
 $M_\infty = 2.3$ , (cf. Ref. 3)

are shown in Fig. 7 (cf. Refs. 3, 4, and 46). Separation ahead of a step is a strong, self-induced interaction flow. The inviscid flow affects the viscous flow and is in return affected by the viscous flow. Thus the separation point is not known beforehand; the flow adjusts itself to an equilibrium position. The reattachment point, on the other hand, must be at the top of the step.

A laminar boundary layer cannot withstand the pressure rise that a turbulent one can, and so separates much further upstream. The effective shape seen by the inviscid flow is a wedge of small slope, as evidenced by the shock wave pattern and by the surface pressure distribution. Turbulent boundary layers separate just ahead of the step and give rise to much stronger shock waves.

As an example, Sterrett and Emery (Ref. 4) state that for identical steps and free stream Mach numbers laminar separation occurred about 17 step heights upstream of the  $\frac{1}{4}$ " step whereas turbulent separation occurred about 4 step heights upstream and had a pressure rise 3 times as great as the laminar pressure rise. Once again transitional separation yields a flow picture and pressure distribution which are composites of the laminar and turbulent cases; the length of the separated flow region is between the laminar and turbulent lengths and the pressure distribution resembles the laminar case. The characteristic plateau prevails up to the transition point, after which the flow resembles the turbulent case. The total pressure rise is between those associated with laminar and turbulent separations.

The turbulent pressure distribution has a characteristic peak prior to reattachment. The peak pressure ratio increases and moves upstream as the step height increases (Refs. 6 and 46). The value of the peak pressure rise coefficient is apparently independent of Reynolds number, as evidenced in Fig. 16 of Ref. 4, Fig. 5 of Ref. 6, Fig. 6 of Ref. 9, Fig. 20 of Ref. 46, and Fig. 1 of Ref. 64.

The peak pressure rise coefficient for turbulent separation ahead of steps decreases with increasing Mach number. Reshotko and Tucker present their analysis of turbulent separation ahead of steps in Ref. 7; they find that the pressure rise ratios should be functions of the Mach number ratio across the inviscid shock wave. For the peak pressure rise ratio the Mach number ratio is 0.762. Their prediction is fairly good for undisturbed stream Mach numbers less than about  $3\frac{1}{2}$ . Mager's work, which involves a Mach number

ratio also, does not depend on geometry and is shown on page 16; for this case the ratio varies from 0.7 to 0.775. Lange's earlier empirical work leads to  $C_{p_{peak}} = 0.52 - 0.09M_{\infty}$  which is in fairly good agreement with the later results of Refs. 4, 7, and 9 for  $1.5 < M_{\infty} < 3.5$ . The following empirical relationships of Love (Ref. 9) and Sterrett and Emery (Ref. 4) adequately predict the peak pressure rise coefficient, which is seen to be independent of the Mach number ratio across the shock;

from Love, for  $1.5 < M_{\infty} < 3.5$ , and  $H > \delta$

$$C_{p_{peak}} = \frac{3.2}{8 + (M_{\infty} - 1)^2}$$

and from Sterrett and Emery, for  $3.5 \leq M_{\infty} \leq 6.5$ , and  $H > \delta$

$$C_{p_{peak}} = 0.13 - \frac{1.5}{M_{\infty}^2} + \frac{9.1}{M_{\infty}^3}$$

Sterrett and Emery mention the important fact that the above equations are only applicable once the step height is sufficiently large to give constant peak pressure coefficients. From the earlier work of Bogdonoff and Kepler (Ref. 46), we conclude that the step height must be larger than the undisturbed boundary layer thickness for the equations to hold.

The separation pressure rise does not depend on the height of the step (cf. Fig. 7 of Ref. 46). Mager's work leads to a Mach number ratio of 0.742 for turbulent separation regardless of the geometry and mechanism causing it (see pages 14 and 15). Because of the steepness of the pressure gradient near separation, it is

hard to determine  $C_{p\text{sep}}$  experimentally. Values of the separation pressure coefficients, obtained experimentally by Chapman, Kuehn, and Larson and Sterrett and Emery (Refs. 3 and 4) are shown in the adjoining Fig. 8.

Laminar separation ahead of a step depends both on Reynolds number and on Mach number. The separation and plateau pressure coefficients are considered by most authors to be independent of the mode of producing separation. Love points out in Ref. 9 that the pressure rise at the laminar foot is independent of geometry but not necessarily the pressure rise at the first downstream peak; however, his curve (Fig. 5 of Ref. 9) suspiciously resembles transitional separation ahead of a step (cf. Figs. 12 and 23 of Ref. 3).

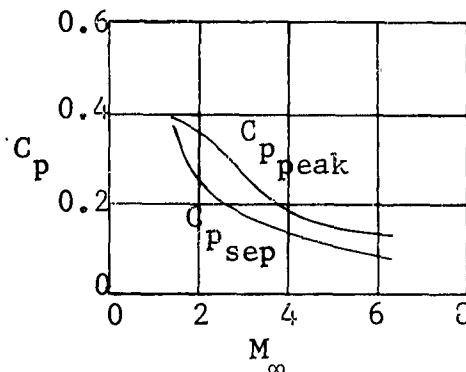


Fig. 8 Pressure Coefficient for Turbulent Separation ahead of a Step

The engineering method of locating the separation point for either laminar or turbulent separation ahead of a step is as follows. The plateau or peak pressure coefficient is found for the prevailing type of boundary layer and local Mach and Reynolds numbers. The oblique shock wave giving the pressure rise and the corresponding deflection of the inviscid stream may be found from tables such as those in Ref. 61. The deflection angle is measured from the top of the step downward to where it intersects the surface upstream of the step. We have found good agreement using this rough method with the recent data from Ref. 4 up to  $M_\infty = 6.5$ .

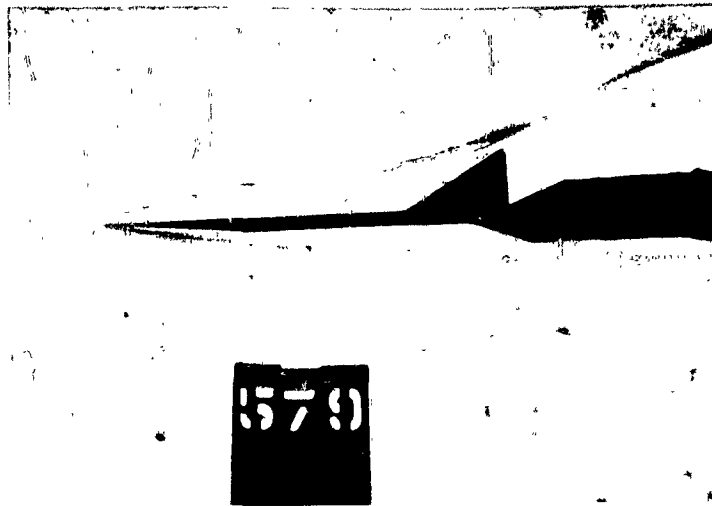
Bogdonoff and Vas describe two important effects related to step separation in Ref. 97. The first concerns the hypersonic blunt leading edge effects. A step on a flat plate "sees" the local flow which may be drastically altered by any bluntness of the leading edge of the plate. They found that the preceding results may qualitatively be superimposed on the blast-wave pressure

distribution that would exist over the plate alone in a hypersonic stream. Secondly, they rounded the step making the step front a hemi-cylinder. The step shoulder was thereby moved downstream and the pressure in the separated-flow region was reduced. The reduction of the pressure is roughly equivalent to the reduction in the blast wave pressure due to the movement of the shoulder downstream, and so no reliable results may be drawn for the effects of rounding the step corner because of the preponderance of the blast wave effect. More discussion of the effects of rounding a step corner is contained in the section on Cavities.

### Ramps

Understanding the flow field ahead of a ramp is important for conventional flap-type controls. Again, the geometric effects are more pronounced for turbulent layers, with the difference between the peak pressures for steps and wedges becoming greater as the Mach number increases. Also, the location of boundary layer transition with respect to the separation and reattachment points significantly affects the pressure distribution (Fig. 1). Schlieren photographs of flow in the Grumman Hypersonic Shock Tunnel in front of a 30° wedge mounted on a 5 inch-long flat plate are shown in Fig. 9 for Mach 13 for Reynolds numbers of  $5 \times 10^4$  and  $20 \times 10^4$ . Note how the rapid growth of the hypersonic boundary layer makes it very difficult to define a separation point, even when optical techniques are used.

Separated flows in front of ramps are complicated by the fact that neither the separation nor the reattachment points are known beforehand. The interaction between the shock wave and the boundary layer adjusts until an equilibrium position is obtained. An estimation of the extent of the separated-flow region may be made as follows. The plateau pressure for laminar separation is associated with a given oblique shock strength and is also a function of the Reynolds number at the point of separation. The flow deflection angle is uniquely determined knowing  $M_\infty$  and  $p_2/\rho_\infty$  for the oblique shock (cf. Ref. 61). The flow angle and the corresponding flow conditions prior to reattachment may be used to determine if the flow will reattach on the ramp. A few iterations may be required to obtain a spread of possible solutions or to ascertain if any solution is compatible for the given flow. If the wedge angle is too high, or the wedge is too short, the flow will



$$Re_L = 5 \times 10^4$$



1581

$$Re_L = 20 \times 10^4$$

Fig. 9 - Schlieren Photographs of Separation Ahead of 30° Ramp,  $M_\infty \approx 13$ , Grumman Hypersonic Shock Tunnel

reattach at the top of the wedge and the flow will be similar to separated flow ahead of a step. For transitional separation the flow is more likely to reattach on a given wedge since the turbulent reattachment criteria can be applied. For turbulent separation ahead of a wedge the pressure distribution exhibits a characteristic "inflection point" at the start of the wedge (cf. Fig. 14 of Ref. 3 and Fig. 7 of Ref. 6). The value of the inflection point pressure coefficient is used in determining the deflection angle of the dividing streamline.

Reshotko and Tucker (Ref. 7) obtain a solution for the inflection point pressure ratio which corresponds to a Mach number ratio across the inviscid shock,  $M_2/M_\infty = 0.81$ . When compared with their solution for steps,  $M_2/M_\infty = 0.762$ , this solution displays the importance of geometry which is ignored in Mager's works (in which, for wedges as well as incident shocks and steps, the Mach number ratio at separation is taken as 0.742). The flow deflection angle may readily be obtained from shock tables using this Mach number ratio of 0.81.

Pressure distributions for  $10^\circ$ ,  $20^\circ$ , and  $30^\circ$  wedges on flat plates, obtained for Mach 11.6 flow in the Princeton helium tunnel, are presented in Ref. 97. The hypersonic blast-wave effects may be superimposed on the pressure distributions for the upstream portion of the flow where separation exists ahead of the wedges. In the interaction region the blunt leading edge effects change the expected pressure distribution radically. For  $10^\circ$  wedges, the thinner the leading edge the thicker the laminar boundary layer and the further upstream separation occurs. The flow field becomes complicated at high Mach number, and it is difficult to assess the extent of separation because of the blast wave and viscous interaction effects. Similar studies were performed on a blunt flat plate with a 25% chord trailing edge flap (Ref. 66). The plate was fixed at zero angle of attack in the Mach 13.4 helium stream and the flap was deflected into the stream at angles up to 20 degrees. Separation occurred at the quarter chord point for the maximum deflection angle.

Curved fillets placed in the corner of a ramp on a flat plate smooth the inviscid pressure rise and make it continuous. Drougge presents experimental evidence in Ref. 8 for which there was no separation of a turbulent boundary layer for pressure rises equal

to  $0.48q_{\infty}$  for stream Mach numbers of 1.81 and 2.76. Although Schuh mentions in Ref. 11 that these pressure rises, being larger than the critical pressure rise, cannot be attributed to the continuous compression, the other authors generally disagree. Typical pressure distributions ahead of a circularly filleted  $25^{\circ}$  ramp are shown in Fig. 17 of Ref. 3. No separation at all was observed in the turbulent case when the ramp was sufficiently filleted.

A theoretical treatment of moderately separated flows due to a prescribed, continuous, (isentropic) pressure rise is presented by Bloom in Ref. 67. The velocity profile is assumed representable by a fourth degree polynomial and the integral method described on pages 206 and 289 of Ref. 1 is used.

### Spikes

Laminar separation may advantageously be used in hypersonic flows, although the use of separation devices, such as spikes, could produce unpredictable forces. The use of spikes in front of blunt axisymmetric bodies to reduce the forebody drag by effectively streamlining the blunt body has been a controversial subject for several years. In the endeavor to better understanding the pertinent phenomena, Bogdonoff and Vas present in Ref. 65 an initial experimental study of two-dimensional spikes in front of hemicylindrical leading edge flat plates. The basic flow phenomena are akin to those ahead of a step although the purely separation flow aspects are somewhat clouded over by the use of small models, necessitated by the Princeton Helium Tunnel, and the importance of the hypersonic blunt leading edge effects.

The defining feature of the spiked bodies is the ratio  $R_a$ , of the length of the thin spike to the thickness of the blunt body (the diameter of the hemicylinder in these cases). Laminar separation near the tip of the spike is observed for  $R_a < 3$ . At greater values of  $R_a$  the separation point is on the surface of the spike but little further change in the pressure distribution over the hemicylinder occurs. The forebody pressure drag is reduced to a very small fraction of that without a spike. In addition to the drag being only a minor portion of the unspiked body (about 10%), the heat transfer to the hemicylinder was reduced to about 30% of the unspiked value. The important requirement for the reduction of the heat-transfer rate is that the boundary layer remain laminar

after separation. Finally, deflecting the spike leads to an effective control device. A larger discussion on spikes is found under Axisymmetric Bodies.

### Separation on Leeward Surfaces

In subsonic aircraft, the sudden loss of lift, or stall, is due to separation on the leeward side of the wing. At hypersonic speeds, however, the leeward side of the vehicle contributes only a minor portion of the lift, so the changes in flow field due to separation on the leeward surface do not result in large changes in aerodynamic loads. We consider these problems because of their importance to heat-transfer distributions and the loss of control effectiveness in regions of detached flow.

This section deals with so-called breakaway separation for which the flow separates from the surface even though the inviscid streamwise pressure gradient is favorable. This phenomenon may be related to the limiting turning angle given by inviscid supersonic theory, but the presence of a thick boundary layer often complicates prediction of the flow. Surface geometry often dictates the existence of breakaway separation, such as from the leading edge of a sharp plate at high angle of attack or from a rearward-facing step or base region. The total separated-flow region with reattachment either in the wake or on the surface must usually be considered in these problems. As in the preceding section, only two-dimensional flows are considered.

There are two factors which contribute to a flow "breaking away" from a surface on which, in the inviscid sense, the streamwise pressure gradient is favorable. High Mach number flows have relatively small maximum turning angles in a Prandtl-Meyer expansion (e.g.  $28^\circ$  for  $M = 10$ ,  $\gamma = 1.4$ ), which result in a predicted cavitation region for surface deflections greater than the maximum angle. This simple phenomenon becomes much more difficult to predict when entropy layers from upstream shock detachment and thick boundary layers create a region of low Mach number flow near the corner. The inviscid cavitation region now becomes a separated region, fed by the low-energy fluid near the wall. Equally important is upstream propagation of the effects of downstream recompression of the flow, sometimes in the wake, but often on the body itself. These two factors are often present simultaneously and are therefore difficult to isolate conceptually.

The flow sketched in Fig. 10 is to be studied under the present contract. Intuitively, the inertia of the flow can cause local separation at the sharp ridge; reattachment is expected upstream of the base of the test configuration. Lessen and Lees (Refs. 68 and 69) note that the centrifugal force acting on the flow must be balanced by the radial pressure gradient and, using standard boundary layer theory, show that even highly cooled boundary layers (for which the mass flow is a maximum near the surface rather than near the edge)

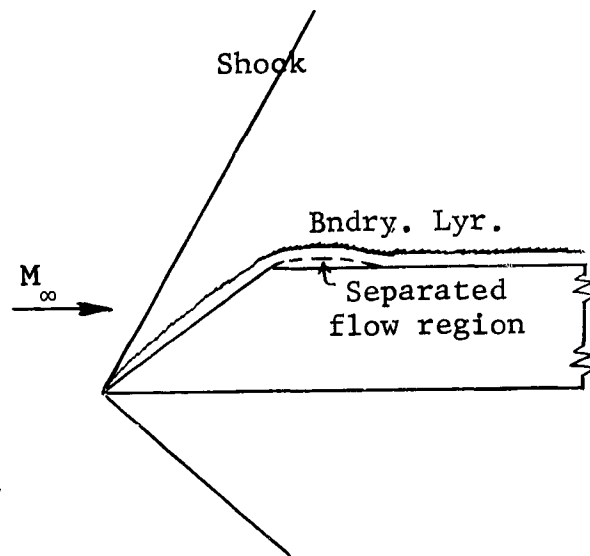


Fig. 10 Breakaway Separation

are always stabilized by convex surface curvature. Interactions of turbulent boundary layers with Prandtl-Meyer expansion fans have been investigated in particular by Murthy and Hammitt (Ref. 70). The failure of present theory to explain the experimentally observed regions of locally separated flows is believed to result from the standard assumption that the boundary layer is thin with respect to the surface radius of curvature; for sharp edges, such as the ones under consideration, the surface radius of curvature vanishes. The complete Navier-Stokes equations must be re-examined for treatment of this problem. A better understanding of the phenomena will facilitate analyzing the general problem where both surface curvature and downstream adverse pressure gradient are important in causing separation.

Leading-edge separation and reattachment on a concave surface are treated by Chapman, Kuehn, and Larson (Ref. 3). Their work is described in Theoretical Approaches. The pressure ratio given by their equation on page 18 was found to be independent of Reynolds number and is in excellent agreement with the experimental data. In applying the method to flows over rearward-facing steps (sketched with pressure distributions in Fig. 11), small errors were to be expected in the results because of the existence of a boundary layer at separation (they assume no initial boundary layer, see page 18). When the transition point was near or upstream of reattachment shocks were noticeable at recompression and the

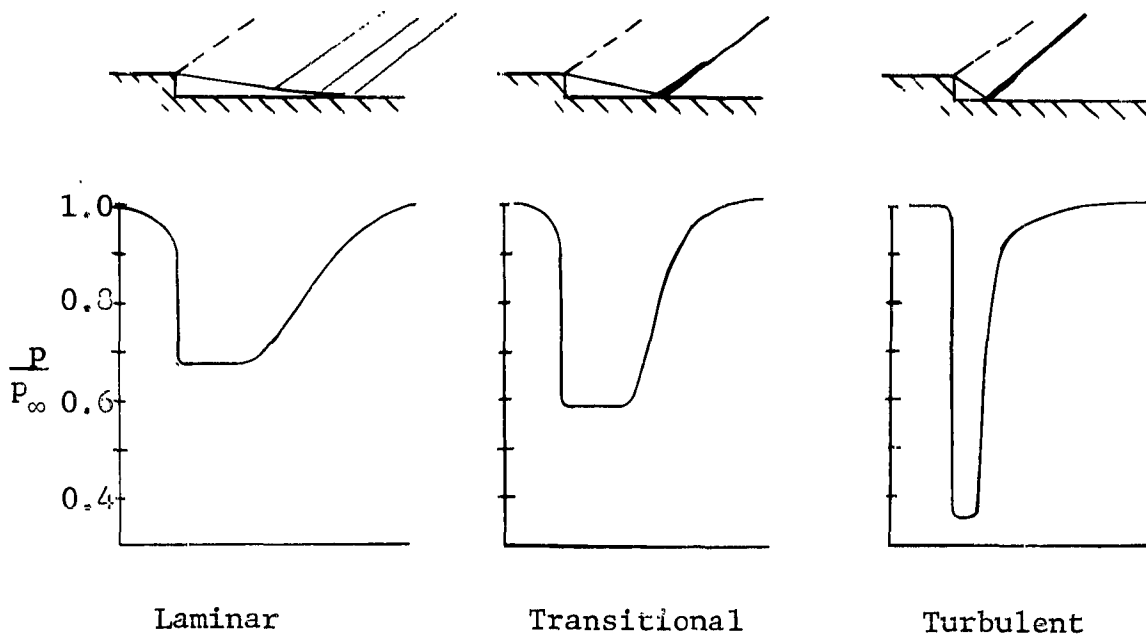


Fig. 11 Flows over Rearward Facing Steps (from Ref. 3)

pressure in the separated region decreased. The separated zone was shortest for turbulent separation and the pressure was only a small part of the laminar separation pressure.

The application of the theory of Chapman, et al., involves an iterative scheme. Beheim describes the scheme in Ref. 71 as follows: first the base pressure is estimated, next the turning angle and Mach number are calculated according to Prandtl-Meyer expansion, and then isentropic compression at reattachment gives the final Mach number and pressure, which must agree with the Chapman reattachment equation presented on page 13. Beheim includes the use of tabulated values of the velocity ratio along the dividing streamline for both laminar and turbulent flows and allows the reattachment surface to be canted up at an arbitrary angle. This method should probably be modified for entropy rise in the recompression when the mixing layer is turbulent.

The importance of the ability of boundary layers to transmit the effects of a pressure rise far upstream is brought out in several reports (cf. Refs. 42, 72, and 73). Love (Ref. 72) assumes the flow behind a blunt-based two-dimensional body to be completely analogous to the flow ahead of a forward facing step, and obtains fair experimental agreement for base pressures for turbulent

boundary layers. The turning angle into the wake behind the blunt body is taken to be the angle corresponding to the peak pressure rise coefficient for turbulent boundary layer separation ahead of a step which is a function of only the free stream Mach number (see the equations on page 28). Evident in the flow photographs presented in Ref. 72 is the existence of a "lip shock" immediately downstream of the expansion fan at the corner of the base. Apparently the flow overexpands slightly and must undergo a compression through a shock wave.

Separation from a smooth surface upstream of the wake is experienced on many lifting surfaces. As the angle of attack increases the critical pressure ratio is exceeded (the trailing-edge shock becomes stronger) and the flow separates before the trailing edge. The extent of the separation increases with the strength of the trailing-edge shock that would be required to turn the flow parallel to the stream. This form of separation, studied, for example, by Ferrari (Ref. 73), is quite similar to separation in over-expanded nozzles (Refs. 42 and 74). If the ambient discharge pressure is larger than the critical pressure, separation will occur in the nozzle. The location of the separation will adjust itself to the point where, for the local value of the Mach number in the nozzle flow and the character of the boundary layer prevailing at that point (laminar or turbulent), the corresponding separation pressure-Mach number relationship is satisfied.

### Three-Dimensional and Unsteady Flows

The preceding sections are limited to descriptions of separation phenomena which are two-dimensional in nature; this section comprises a discussion of three-dimensional and unsteady flow phenomena associated with separation. Three-dimensional flows have been observed occasionally over two-dimensional forward and rearward facing steps (Refs. 4 and 75). Sterret and Emery note that the flow ahead of a step has a three-dimensional character whenever transition is close to the point of separation (Ref. 4); the same type of flow is observed by Chapman, Kuehn, and Larson for lower stream Mach numbers (Ref. 3, Fig. 35). In the latter case it is noted that the peak pressure rise measured is considerably less than the theoretical two-dimensional value. Kline (Ref. 76) suggests that the inception of stall in turbulent boundary layers cannot be described by any two dimensional flow model. Separation, according to his thesis, comes about through the non-steady appearance of stall in a sublayer produced by an adverse pressure gradient. This would mean that turbulent boundary layer

separations can be microscopically three-dimensional even if the surrounding geometry is two-dimensional. Unsteadiness of a comparable magnitude must accompany this effect.

Although the detailed physical process of separation is probably three-dimensional, even for essentially two-dimensional boundary conditions, two-dimensional flow models are amenable to analysis and the methods described in the preceding sections enable one to predict roughly the separation flow phenomena on many practical geometries. Even truly three-dimensional flows, such as separation ahead of a swept step, may be analyzed by considering the component of the flow normal to the step. Macroscopically three-dimensional separation and effects of flow fluctuations are described in this section. Particular three-dimensional and unsteady flow effects pertinent to cavities are described in the following section Flow Over Cavities.

In view of the general lack of solutions to three-dimensional boundary layer problems, it is even more difficult to give specific information about three-dimensional separation than it is in the two-dimensional case. There are, however, certain special characteristics of three-dimensional separation problems which should be discussed. (Three-dimensional here implies axially non-symmetric.)

First, the problem of the definition of separation is more complex than before. Several authors (cf. Sears, Ref. 77 and Moore, Ref. 78, page 202) have discussed various approaches to defining these separation phenomena. We feel that the best definition for a specific problem must be the one which deals with the flow variables of importance to that problem. One basic criterion which is often useful is the existence of a dividing stream surface (either closed or open to the wake) across which there is no net macroscopic mass flow. Another definition uses the locus of points of vanishing wall shear stress. Although both of these ideas are useful for certain problems, each can be misleading when applied to other problems of practical importance.

Secondly, we must expect the increased geometric flexibility of three-dimensional flows to cause novel behavior of the flow. For example, the requirement of zero velocity everywhere on a surface leads directly to the fact that wall shear stress must always vanish at perpendicular and acute intersections of plane walls,

and this leads to the immediate onset of separation in the presence of adverse pressure gradient. Here we also see the latter of the suggested definitions failing, as it indicates that a streamwise corner boundary layer is always separated even in a favorable pressure gradient (Ref. 79). It is also possible in many three-dimensional flows for one flow component to separate while the other remains attached. This can lead to large increases in separation-zone pressure and heat-transfer rate because the changes in effective body shape and convection in the boundary layer affect a more energetic flow.

The three-dimensional separation problems most important to control effectiveness are those of "swept" oblique shock interaction, venting of the low-energy separated flow at the spanwise extremity of a two-dimensional separation, separation in the presence of crossflow, and separations along intersection lines. Of these, the first appears to be amenable to approximate solution using a simple analogy to two-dimensional shock-induced separation in shock coordinates. Theoretical and experimental research on this problem is being conducted under the present contract. An indication of the importance of this type of separation can be gained from investigation of Fig. 12; the pressures on a flat-plate  $65^\circ$  delta wing are greatly altered by separation induced by the shock from an underslung cone body. The data shown are typical of the results of tests performed at Mach 5.1 and 8.1 in AEDC tunnels A and B [AF Contract AF 33(616)-6400, Ref. 80].

The simplest approach to three-dimensional flows ahead of steps is to consider only the component of the flow normal to the step. Stalker does this for turbulent boundary layer separation (Refs. 81 and 82). The spanwise component of the flow affects neither the reattachment line position nor the peak pressure rise for sweepback angles less than about 45 degrees. So also, the pressure rise at reattachment is not influenced by the spanwise component of the flow; the reattachment line is parallel to the rearward facing step. The effects of sweepback on shocks incident to turbulent boundary layers are similarly considered by Gadd (Ref. 47).

In many problems of practical importance spanwise flow into or out of a separated region has very large influence on the flow characteristics in the entire separated region. The shape of a two-dimensional separation zone is in a large part dependent on

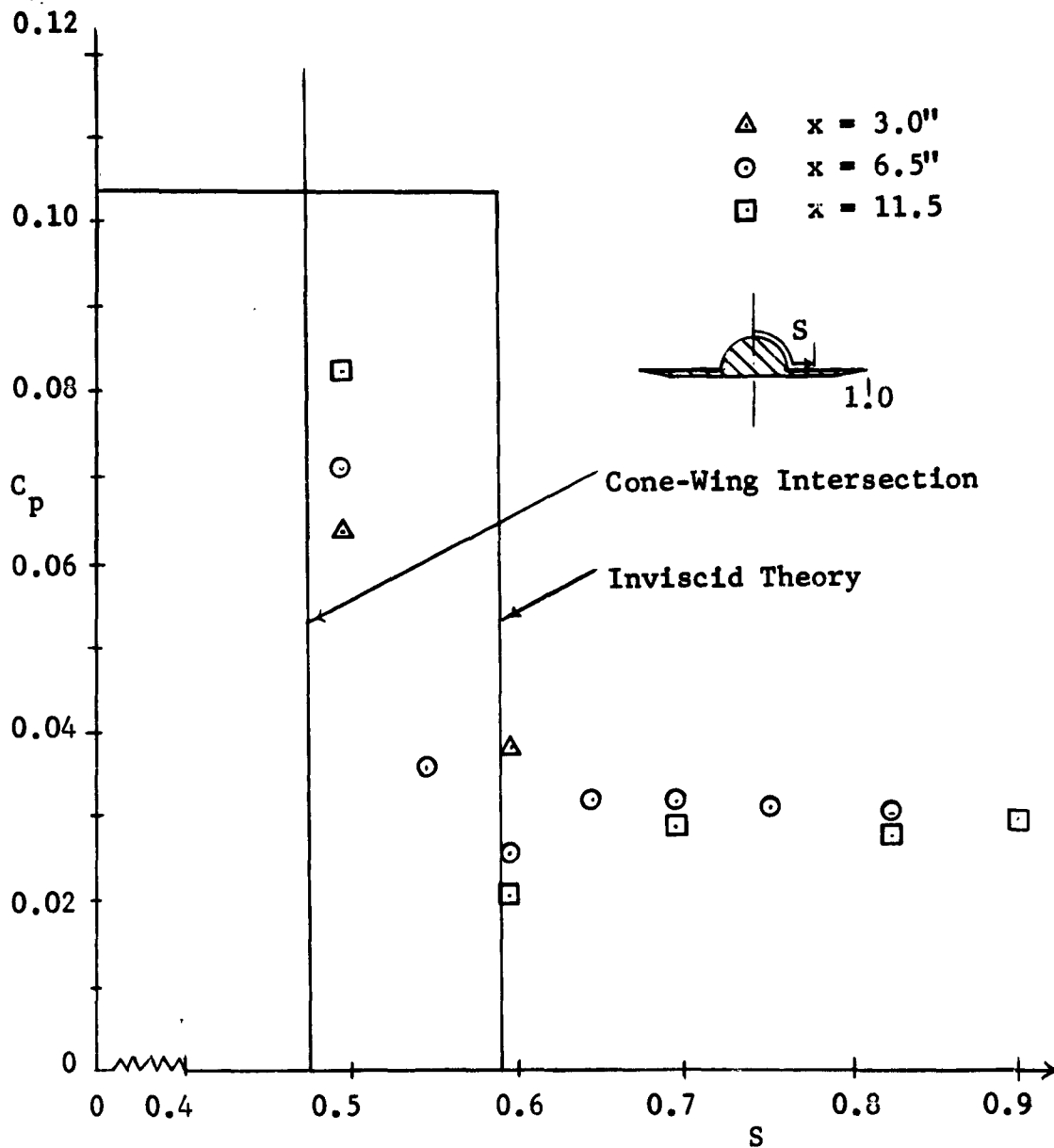


Fig. 12 - Pressure Distribution near Wing-Body Intersection at Hypersonic Speeds (Flat-Plate,  $65^\circ$  Sharp-edged Delta Wing,  $12.5^\circ$  Half-cone Body,  $M_\infty = 3.1$ ,  $\alpha = 0$ ,  $Re_L = 3.3 \times 10^6$  (Data from Ref. 30)).

trapping of the fluid within the envelope of the dividing streamline. The low-momentum fluid in the separated zone responds readily to any lateral pressure gradients which exist, and large changes in separation pressure distributions can thereby result, because the effective body shape is altered. We know of no available methods for estimating the magnitude of this effect, but it is being investigated theoretically and experimentally under the present contract. The obvious importance of chord-to-span ratio of the separated region must be considered, with a possible dependence on the average height of the separation zone as well.

- Separation in the presence of crossflow is an unsolved problem for both laminar and turbulent flow, but it does appear likely that in certain situations the crossflow effects can be decoupled from the main-flow component. Citing the above examples of the swept oblique shocks, one can consider these examples of pseudo-two-dimensional separations with very strong crossflow. This case shows little effect of the flow parallel to the shock, probably because the flow parameters change slowly along the shock. Because of this, the coupling between the two components of the vector equation of motion parallel to the surface is very weak, and the two-dimensional separation phenomena can be considered separately from those of the streamwise flow. All velocity components must be considered for the energy equation, but this is straightforward if one is willing to accept reasonable approximations. Similar decoupling of the flow components should be possible in other problems of separation with crossflow. Summaries of recent methods of treating three-dimensional boundary layers by decoupling crossflow equations are presented in Refs. 83 and 84.

Flow along a streamwise intersection is extremely susceptible to separation, as mentioned previously. Although shock interactions will often predominate over corner boundary layer effects in hypersonic problems, it is important to understand the phenomena involved. Bloom and Rubin give a good summary of the subject (Ref. 85). Incompressible experiments, presented in Ref. 79, help to give an understanding of corner separation under adverse pressure gradients. Some questions concerning the development of a momentum integral theory for the case of a nonuniform free stream flow have still not been answered. These points are discussed in Ref. 79, and probably apply as well to the high-speed case.

Another three-dimensional separation problem which should be mentioned is the case of an external corner or edge such as a truncated wingtip. Inviscid phenomena usually predominate in such flows, but as far as the viscous contributions are concerned, these boundary layers show an increased resistance to separation. This is in accord with the decreased separation resistance of internal corners. Some recent work by Stewartson and Howarth (Ref. 86) has contributed to the understanding of these flows for zero streamwise pressure gradient. An important result is that the transverse momentum exchanges are important even to flows parallel to an edge, and the problem solution must therefore consider in some way all of the components of the vector equations of motion. This result also holds for the internal corner problem.

Heat-transfer rates and wall shear forces are greatly altered near separation and reattachment points by macroscopic flow fluctuations because of the Reynolds stress effect. An order of magnitude estimate (due to C. Donaldson) of these increases can be obtained in the following way. The average Reynolds stress can be written as  $\tau' = \rho \overline{u'v'}$  and the incremental pressure change due to the flow fluctuation, obtained from supersonic linear theory, is  $\Delta p = \frac{\rho u^2}{\sqrt{M^2-1}} \left\{ \frac{\Delta v}{u} \right\}$ . Combining these equations with the momentum equation, the Reynolds stress becomes  $\tau' = \frac{(\Delta p)^2 \sqrt{M^2-1}}{\rho u^2}$ .

Correlation of experimental and theoretical data indicates that the pressure differential at the separation point can be written as  $(\Delta p)_{sep} = \frac{n \rho u^2 \sqrt{C_{f_0}}}{(M^2-1)^{\frac{1}{4}}}$ , where  $n$  is an empirical correlation

constant,  $n \approx .66$  for laminar and  $.35$  for turbulent flow. The skin friction coefficient due to the Reynolds stress can then be written as  $C_{f'} = C_{f_0} n^2$ . An estimate of the aerodynamic heating rate can be obtained if we assume an enthalpy distribution of the form

$$\bar{i} = (i + i') = i_w + (i_{aw} - i_w) \left\{ \frac{u}{u_w} + \frac{\bar{u}'}{u_e} \right\} - (i_{aw} - i_e) \left\{ \frac{u}{u_e} + \frac{\bar{u}'}{u_e} \right\}^2$$

and

$$i = i_w + (i_{aw} - i_w) \left\{ \frac{u}{u_e} \right\} - (i_{aw} - i_e) \left\{ \frac{u}{u_e} \right\}^2$$

The aerodynamic heating rate can be written as  $\dot{q}_w' = - \frac{k_w}{C_{p_w}} \left\{ \frac{\partial i}{\partial u} \right\}_w \left\{ \frac{\partial u}{\partial y} \right\}_w$ . Applying this equation to the steady and unsteady terms, and assuming a constant Prandtl number, we obtain

$$\frac{\dot{q}_w'}{\dot{q}_w} = \frac{\tau_w'}{\tau_w} = \frac{C_{f'}}{C_{f_0}} = n^2. \text{ This relationship enables us to estimate}$$

the increase in heating due to oscillations when the equivalent heating rate for steady flow is known, and it should be reasonably correct for both laminar and turbulent flows if the proper value of  $n$  is used. Theoretical analyses of the oscillations and stability of shock waves interacting with boundary layers are presented in Refs. 87 and 88; experimental verification of the theoretical results is presented in Ref. 89. The results of investigations of unsteady flows over cavities are described in the following sub-section.

### Flows Over Cavities

Flows over cavities, occasionally referred to as "ditches" or "notches", have received much recent attention (cf. Refs. 14 and 90 through 94). Small surface cavities (such as that ahead of a flap) may drastically affect the aerodynamic characteristics of a hypersonic vehicle. Indeed, structural failure in a hypersonic flight vehicle has been attributed to the unsteady flow that existed in a cavity on the vehicle surface (Ref. 93). On the other hand, it is thought that cavities may prove to be useful as drag-generating devices for re-entry bodies (Ref. 91). Investigations of separation phenomena for flows over cavities are somewhat simplified in that the extent of separation is fairly clearly

defined. Thus, much of the experimental research on temperature and heat-transfer effects on separation has been accomplished using both axisymmetric and essentially two-dimensional models with surface cavities (Ref. 14 and 92). Different types of two-dimensional cavity flows that have been observed, along with their typical pressure distributions, are sketched in Fig. 13.

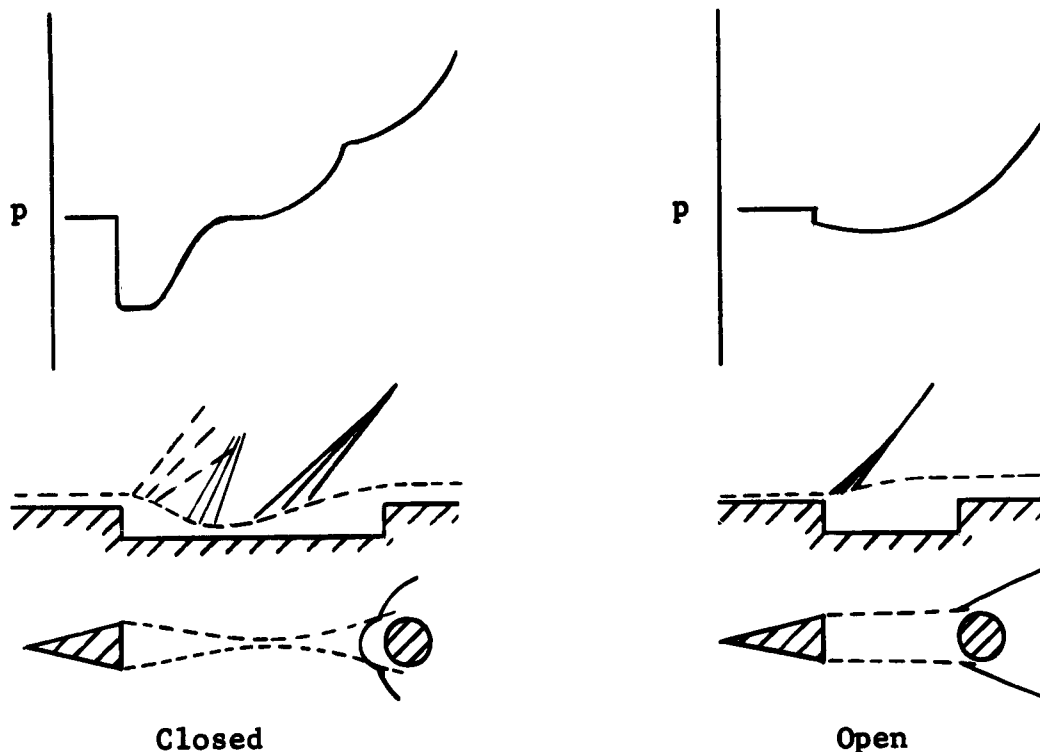


Fig. 13 Cavity Flows (from Ref. 90)

A plane of symmetry for free cavity flows replaces the floor of bounded cavities. It is understood that we are referring to bounded cavity flows unless otherwise specified. When the dividing streamline is coincident with a segment of the cavity floor, the cavity flow is called closed. For open cavity flows the dividing streamline "bridges" the cavity. For equal depths, longer cavities will be "closed" and shorter ones will be "open". The length of a cavity is properly defined as the distance from the separation point to the shoulder of the recompression side of the cavity.

Free cavity flows were investigated experimentally using a cylinder placed in the wake behind a wedge (Ref. 90). The cylinder was moved fore and aft a sufficient distance to insure obtaining both open and closed flows (cf. Fig. 13). When the cylinder is far downstream of the wedge, there is a typical wake flow behind the wedge, similar to those behind blunt bases and rearward facing steps, and the flow over the cylinder is much the same as it would be in the free stream. There is a strong, curved shock ahead of the cylinder and the maximum surface pressure is on the center line. As the cylinder is moved upstream the bow shock wave in front of it develops a bulge which is found to contain a pair of vortices. Maximum pressure points are measured near the sides of the cylinder rather than on the flow center line. As the distance between the cylinder and wedge continues to decrease, the wake flow behind the wedge interacts with the vortical flow ahead of the cylinder until finally, below some critical value of cavity length-to-height ratio, the wake opens.

Flows over bounded cavities exhibit identical phenomena. For long cavities there are reverse flow regions both immediately behind the rearward facing step and in the separated flow region in front of the forward facing step. The vertices of the two separated flow regions approach one another as the cavity length is decreased. The cavity flow opens when the vertices meet so that the reverse flow in front of the step flows into the wake region. Backflow occurs from the recompression region to the separated wake region.

The critical length of a cavity, sometimes referred to as the critical closure distance, is the length for which the cavity flow is just closed. At this condition the vertices of the separated flow regions just coincide. Any reduction in the cavity length below the critical value will cause open cavity flow. A simple expression for the critical length in terms of the lengths and heights of the separated regions in the closed cavity flow is (Ref. 90):

$$\frac{L_{crit}}{H_1} = \frac{L_1}{H_1} + \frac{H_2}{H_1} \left\{ \frac{L_2}{H_2} \right\}$$

where the symbols, for the above equation, are defined in the adjoining Fig. 14. Experimental data for critical lengths correlated quite well using the above equation, which is plotted in Fig. 14. Data were obtained for turbulent boundary layers ahead of both two-dimensional and axisymmetric cavities; the critical lengths are independent of Mach number and the shape of the recompression step (flat, wedge, and circular steps were used). The spread of experimental data about the correlation curve shows a certain hysteresis effect; i.e., the closure of open cavity flows occurs at a different value of  $L_{crit}$  than the equivalent opening of closed cavity flows. This effect is more pronounced for axisymmetric than for two-dimensional flows. For both types of flows, the hysteresis effect becomes more pronounced as the depth of the cavities decreases below the thickness of the undisturbed boundary layer and as the ratio of the step heights varies from unity. There seems to be a definite need for stability analyses of such flows. Indeed, because of the common observance of three-dimensional and unsteady effects in all cavity flows, it is almost fortuitous that two-dimensional analyses are useful at all.

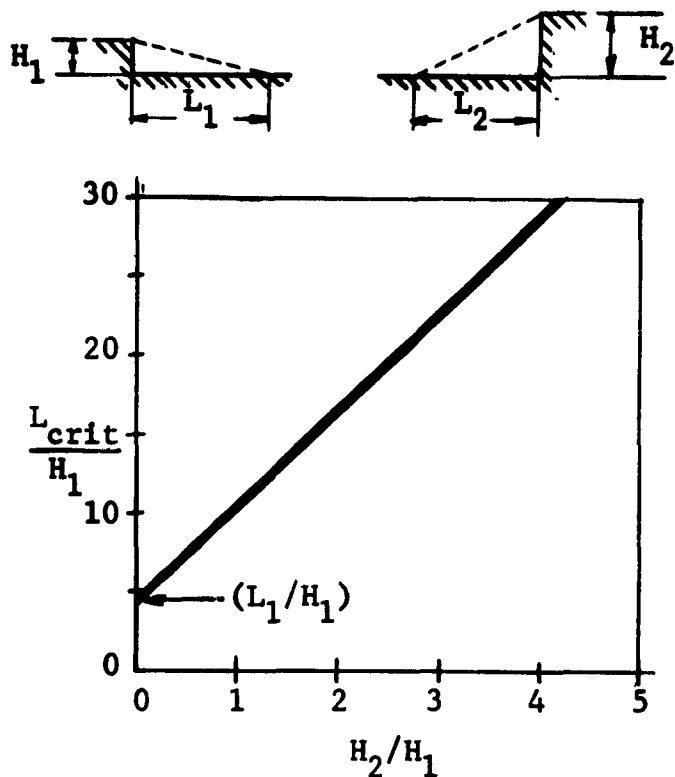


Fig. 14 Critical Lengths for Cavity Flows (Ref. 90)

A possible practical application of cavities is as a drag generating device for hypersonic vehicles. Heat-transfer and drag data for notched bodies of revolution indicate that the cavities greatly increase the drag over that of the smooth bodies but at worst only moderately increase the average heat-transfer to the bodies; thus, the axisymmetric cavities substantially reduce the

average heat transfer per unit drag (Ref. 91). The average heat transfer to the surface for open cavity flow, for cavity depths greater than the boundary layer thickness, is about half that on a corresponding smooth wall. Only for very shallow cavities is the average heat transfer increased slightly above the smooth-wall value. The drag of a notched body, however, for open cavity flows, is an order of magnitude greater than that of the smooth body. For the notched surfaces considered (short enough to have open cavity flow), the great increase in drag led to the result that the average heat transfer per unit drag to the notched wall was about one-twentieth of that of a smooth wall.

Heat-transfer experiments were conducted on axisymmetric and essentially two-dimensional flows over models with and without surface cavities in order to substantiate the theoretical results presented on pages 19 and 20 (Refs. 14 and 92). The tests were conducted in supersonic flows with free stream Mach numbers up to four. The sharp internal corners of the two-dimensional and axisymmetric cavities were filleted in some instances, with negligible effect on the measured heat-transfer rates. For two-dimensional flows, the average heat transfer to the cavity for separated laminar boundary layers was about 56% of the average heat transfer to the equivalent portion of the smooth surface with an attached laminar boundary layer. This value was found to be independent of both Mach and Reynolds numbers and was in excellent agreement with the theory. The average heat-transfer rate to the cavity for turbulent boundary layers was about 60% of the value of the attached turbulent boundary layer. As noted on page 20, this result contradicted the theoretical prediction that separation of a turbulent boundary layer would greatly increase the average heat-transfer rate. The average heat transfer to the axisymmetric cavities followed the same trend as for the two-dimensional flows; for both laminar and turbulent separation the average heat transfer is about 60% of that for attached flows. The heat transfer in the immediate vicinity of reattachment, however, is two to three times larger than that of the attached flow at the corresponding point on the surface, and moreover, remains higher far downstream of reattachment. Thus, when considering separation to reduce heating, although the large heat-transfer rates for the initial portions of attached boundary layers may be greatly reduced, allowance must be made for the higher heat-transfer rates at and downstream of reattachment. As Sprinks (Ref. 56) and several others emphasize, there are no adequate theories and few empirical data for the effects of separation on temperature and heat

transfer; even less is known about the effects of temperature and heat transfer on separation.

A notable difference between separated and attached laminar boundary layers is that transition in the separated layer is moved upstream by cooling the wall. For marginally open cavity flow, cooling the wall causes the flow to close so that the flow is attached on part of the cavity floor. As for attached boundary layers, the stability of laminar layers increases with stream Mach number. Another observed aspect of the stability of separated laminar boundary layers is that cavity flows exhibit an important unsteady resonance effect which can greatly decrease the value of the transition Reynolds number (Ref. 92).

Experimental investigations of resonance effects were made using rectangular cavities in a flat plate and in the cylindrical portion of an ogive cylinder (Refs. 93 and 94). As expected, the pressures on the cavity floors dropped below the stream value near the front of the cavity and increased to yield positive pressure coefficients near the end of the cavity; the distributions were similar to the "open" cavity flow pressure distribution sketched in Fig. 13 on page 44. The variation of the pressure coefficient away from zero decreased as the Mach number increased from 2 to 5 so that, at Mach 5,  $C_p \approx 0$  throughout the cavity. The frequencies of the unsteady flow, which have been responsible for structural failure in cavities in flight vehicles, are inversely proportional to the length of the cavity for all stream Mach numbers (Ref. 93). The frequencies are conveniently presented in nondimensional form using the Strouhal number ( $St \equiv (\text{frequency}) \times (\text{cavity length}) / (\text{free stream velocity})$ ).

### Axisymmetric Bodies

The review of separation phenomena associated with flows over axisymmetric bodies commences with the apexes of the bodies and concludes with their bases. Flow separation spikes, separation ahead of conical flares, and axisymmetric base flows are described in the listed order.

Flow separation spikes, mounted in front of blunt bodies, may possibly be used to effectively streamline the body, thereby reducing the heat-transfer rate and drag of the body (Refs. 95

through 98). The flow separates on the spike ahead of the blunt body in much the same manner as flow separation ahead of a step. Thence, according to the length of the spike with respect to the diameter of the body, the effective nose shape of the body is changed to a more pointed, higher fineness ratio nose, which is essentially conical. The early experimental work of Stalder and Nielson (Ref. 95) gave results which were disheartening at first glance. The pressure drag was reduced by as much as 45% but the corresponding average heat transfer to the nose was approximately doubled. The increase in heat-transfer rate to the forward portion of the blunt body when the spikes were used was due to the transition of the separated boundary layer. It was turbulent when it reattached, and thus resulted in higher heat-transfer rates than did the laminar layer that existed on the blunt body alone. The later experiments of Bogdonoff and Vas (cf. Refs. 96 and 97) clearly indicate that the separated layer may sometimes remain laminar and therefore greatly reduce the average heat transfer to the nose. The spikes used by Bogdonoff and Vas are sharp, needle-like, cone cylinders with diameters very small in comparison with the diameter of the blunt body. The blunt bodies are hemisphere-cylinders and flat-nosed cylinders. The important parameter to be varied is  $R_a$ , which is the ratio of spike length to body diameter. High-speed oscillations of the nose shock (frequencies of about 10 kc) were observed for values of  $R_a$  less than about 3. The shock moves forward with the tip of the spike for these small  $R_a$  values. Around  $R_a = 4$ , the flow separates from the surface of the cylindrical portion of the spike, and continues to do so as the spike length is extended still further. Examples of the drag and heat reduction possible, although the data are from Mach 14 tests in helium, are: for a hemisphere cylinder with a spike having  $R_a = 4$ , the form drag is one-tenth and the average heat transfer one-third of those for the body without a spike; for a flat nosed cylinder with the same  $R_a = 4$  spike, the form drag is one-fortieth and the average heat transfer one-half of the "unspiked" values (Ref. 96). Lynes and Schaaf present their experimental results of spiked bodies in Ref. 98. A hemispherically capped cylinder is moved in and out through a conical frustrum of  $45^\circ$  semivertex angle in a Mach 5.9 air flow. The entire flow is initially separated between the hemisphere and the cone, but as the hemisphere cylinder is pushed out, separation then occurs at the shoulder of the sphere until for greater cylinder lengths the flow separates from the surface of the cylinder. Reattachment is close to the base of the cone. It is noted that

no hysteresis in the location of separation was found as the cylinder was pushed out and then returned to the same position; stability of the separated flows, at least macroscopically, is thereby indicated.

Work of a similar nature is known to be under way by Chapman and his co-workers at the NASA Ames Research Center. A considerable range of Mach and Reynolds numbers is being employed in tests of blunt, axisymmetric bodies with and without spikes. In general, it appears that spikes will provide a considerable degree of drag and heat-transfer reduction, and a simple means of producing large control forces in certain specific applications (primarily laminar flow). Certain conditions produced large-scale unsteadiness which would be catastrophic in a flight vehicle, indicating that considerably more work is necessary before this interesting approach can be properly exploited.

Extensive flow separation may occur ahead of conical flares, such as those commonly employed in multistage rockets, and drastically affect the aerodynamic characteristics of such vehicles. Structural simplicity and aerodynamic stability considerations for Saturn type configurations led to the use of cylindrical segments joined by conical flarings. Hence, there is much current interest in investigating high-speed flows over these configurations (cf. Refs. 99 through 101). Separation in the axisymmetric cylinder-cone compression corners can substantially alter the heat transfer and drag of the vehicle, can cause drastic shifts in the center of pressure, and, if unsteady, can cause catastrophic oscillations. Reattachment near the bases of the conical frustums can cause extremely high local heating. As for two-dimensional separated flows, the character of the boundary layer is most important in determining the region of separation and must be accounted for in any wind tunnel investigations. Laminar separation may be expected far upstream of the cylinder-cone junction whereas the extent of turbulent separation would be much smaller with smaller changes in the inviscid pressure distribution. The unsteadiness of transitional separation must be avoided, perhaps by forcing early transition. Separated flows ahead of conical flares are qualitatively comparable to separated flows ahead of two-dimensional ramps; quantitative results or comparisons are still not available.

Base flows, as considered herein, include flows over rearward-facing axisymmetric steps and conical frustums. The afterbodies may be cylindrical, such as the one on the Project Mercury capsule, or may be conical, representative of rocket engine nozzles. Large aerodynamic loads and high heat transfer result from reattachment of separated flows on such afterbodies which must be designed and constructed accordingly (cf. Refs. 53, 71, 72, and 102 through 104).

Flows over blunt based cylinders with conical or cylindrical afterbodies are analagous to two-dimensional flows over rearward facing steps. The flow separates from the cylinder, passes through an expansion fan, is compressed and reattaches on the afterbody (Ref. 71). The pressure distribution along the afterbody is similar in shape to that for turbulent boundary layer separation ahead of a two-dimensional ramp or step. Although measured pressures are consistently higher than would be expected downstream of reattachment through conical shocks, they are closer to the conical shock solution values than to the higher values associated with two-dimensional oblique shocks turning the flow through the necessary angle. Also, the pressure rise extends over a longer region than would be expected. The recompression is probably somewhat isentropic; compression waves coalesce near the afterbody to form the conical shock. Assuming reattachment through a conical shock, the greater turning angles required by thinner afterbodies lead to higher reattachment pressure values on the thinner afterbodies. Experimentally, however, it is observed that, for  $M_{\infty} = 2$ , the pressure downstream of reattachment on cylindrical afterbodies is approximately 1.9 times as large as the base pressure on the rearward facing step regardless of the thickness of the afterbody (Ref. 71).

Wakes behind axisymmetric bodies without afterbodies are also conical in nature. Weaker lip shocks (cf. p. 37) are observed for axisymmetric than for two-dimensional base flows. The conical expansion angle increases quickly from about  $2^{\circ}$  for  $M = 1$  to a constant value of about  $13^{\circ}$  for  $3 < M < 8$ . The separated flow in the base region may be analyzed using the empirical expansion angle for conical flows or, more simply, using Prandtl-Meyer expansion for an equivalent two-dimensional expansion angle which, empirically, is about 85% of the conical angle (Ref. 72). Although data are scarce, empirical analyses are available for estimating the effects of forebody fineness ratio, boattailing, fins, and angle of attack on base flows (Ref. 72). Few data are

available for heat-transfer rates in wakes behind axisymmetric bodies (Ref. 102).

### Experimental Techniques

Because of the lack of dependable theoretical methods, experiments are of paramount importance in investigations of separated flows. Most of the theoretical methods in use rely to some extent on empirical knowledge, and design calculations must invariably be supported by experimental verification for the specific situation involved. Particularly for separated flows is it advisable to employ a few different types of experimental techniques for the same situation: static pressure measurements, boundary layer probing, skin friction measurements, adiabatic wall temperature measurements, china clay or oil film or droplet techniques, shadowgraph observations, schlieren photographs, high-speed motion pictures, and others.

Static pressure measurements give an indication of the type of separation and the regions of separation and reattachment, but it is often quite difficult to determine experimentally the extent of separation with static pressure measurements alone. The use of other experimental techniques to complement static pressure measurements is particularly important in the case of laminar boundary layer separation. The small pressure rise required to bring about laminar separation is not readily detected; particularly in the presence of other effects, such as blast wave or viscous interaction effects, which are prominent in low-Reynolds high-Mach number flows, the separation zone might be obscured. Pressure distribution measurements can, however, bring out many salient features of the flow and are a must in any comprehensive investigation of separated flows.

Probing the boundary layer is tedious and rather prohibitive for a large scale investigation. In employing this technique, we rely on past experience in knowing the shape of the velocity profiles for laminar, turbulent, and separated flows and thus determine from velocity profiles the nature and location of separation and reattachment. "T" probes may be used to simultaneously measure the streamwise and also the reverse flows. If we are interested in locating just the point of transition from laminar to turbulent, we can do so by placing a total pressure probe near the wall.

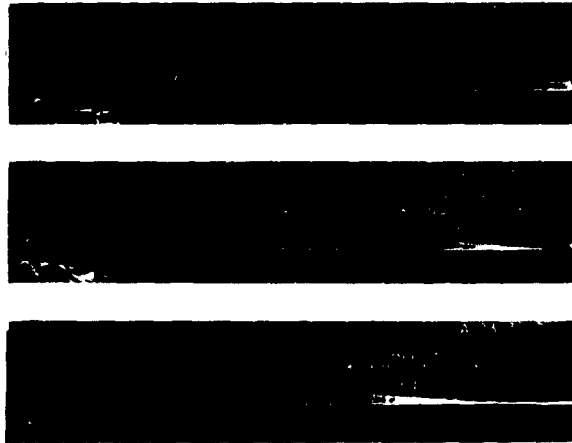
When transition occurs, the pressure reading jumps because the velocity head is higher near the wall for a turbulent boundary layer. Of course, caution must be exercised to place the probe in the appropriate location where the difference in velocity head between the laminar and turbulent layer is more pronounced (cf. Ref. 106).

Skin friction measurements can be made either directly by using a floating element or indirectly by probing the boundary layer. The floating element technique, however, also becomes tedious. One may calibrate a Stanton tube versus a floating element and use the Stanton tube as a skin friction measuring device (cf. Ref. 35). Knowing the skin friction, we can determine the nature of the boundary layer and the points of separation and reattachment.

Temperature and heat-transfer measurements may also be used in determining the nature of the boundary layer. Their use for determining regions of separated turbulent flows, however, is severely limited due to the lack of understanding of temperature and heat-transfer effects (cf. pp. 19 and 47). China clay, oil film, or oil droplets may be used to determine the extent of separation because of the reverse flow near the wall in separated flow regions.

The shadowgraph technique is quite useful in distinguishing laminar and turbulent boundary layers and in determining the region of transition (cf. Refs. 3, 4, and 107 through 109). In brief, at low static tunnel pressures and small film-to-model distances, transition occurs at the end of the so-called laminar white line (which is described in Fig. 15 on the following page). At high tunnel static pressures with small film-to-model distances, or arbitrary tunnel pressures but large film-to-model distances, the laminar white line appears displaced from the surface by a large distance compared to the boundary layer thickness  $\delta$ . This displacement is almost constant for laminar flat-plate flow. As the Reynolds number increases to the point where transition begins, the white line starts converging on the surface and appears tangent to the surface when transition is completed.

Lastly, we mention that from high-speed motion pictures, we can get a qualitative picture of the flow field and determine the steadiness of the separated region. Shock waves interacting with



Examples of Laminar White Lines (From Ref. 3)

The shadow effect responds approximately to second derivatives of the density with respect to the axes perpendicular to the light beam. The laminar white line corresponds, therefore, to the negative second derivative in density that exists at the edge of a laminar boundary layer. For turbulent boundary layers the negative second derivative has smaller absolute value and is found to be near the wall. Hence, the convergence of the laminar white line to the wall and its disappearance at the wall in the turbulent zone.

Fig. 15 - The Laminar White Line

boundary layers are not necessarily stable but oscillate about a mean position (Refs. 87 and 88). Frequencies may be of the order of 2,000 cycles per second (Ref. 89) which can be stopped using high-speed motion pictures of either the shadowgraph or schlieren fields.

This short presentation is included here as an introduction to experimental techniques used in separated flow investigations and is not by any means exhaustive. For further information on the topics mentioned and others, the cited references should be consulted.

## INFLUENCE OF SEPARATION ON CONTROLS

Control characteristics, particularly at hypersonic speeds, are often greatly affected by separation. Control effectiveness may be increased, limited, or may be completely nullified because of boundary layer separation. Pressure distributions over controls and on the basic configuration may be greatly altered due to separation effects, changing drastically the moment coefficients predicted by inviscid theory. Heat-transfer rates are changed on the control surfaces and on the basic configuration both upstream and downstream of the control. Separation effects must therefore be considered in both the design and location of controls. In general, separation tends to smooth out the sharp changes in pressure distributions predicted by inviscid theory, and can cause local "hot spots" which have heat-transfer rates many times higher than those that would exist for attached boundary layers. Separated flow phenomena are frequently unsteady and three-dimensional in nature, and undergo large changes with transition from laminar to turbulent flow, further complicating the analytical treatment of a design. Thus, for example, hysteresis effects are noticeable in the  $C_m$  versus  $\alpha$  curves for some control configurations.

Aerodynamic forces and moments on a vehicle may be changed as much by changing the pressure distribution on the basic configuration as they would be by changes in the normal forces acting on controls. Leading edge controls, for example, usually are not directly influenced by separation but, by causing separation, they can affect the pressures and heat-transfer rates over the entire configuration. Some effects of separation associated with controls on windward and leeward surfaces are described below. Important three-dimensional and unsteady flow effects of separation on control characteristics are presented at the conclusion of this short section.

### Leading-Edge Controls

Leading-edge controls contemplated for hypersonic vehicles include flaps, spoilers, fins, spikes, and all-movable noses. The importance of separation for such controls is in the influence

on the entire flow field downstream of the control. Separation behind a deflected leading-edge flap makes any control or stabilizing surface downstream of the flap ineffectual. Heat-transfer rates on the surface are reduced in the separated-flow region, but if the boundary layer reattaches on the surface the heat-transfer rate at reattachment can be several times larger than that for an attached boundary layer. The control forces and hinge moments of leading-edge fins and flaps would not be directly influenced by separation. Fins, which may be canards, create strong vortices which can cause boundary layer transition and contribute to the possibility of unsteady flow over the downstream surfaces of the configuration. Comparable effects would be expected for large amounts of all-movable nose deflection which, nevertheless, is anticipated to be a very effective trimming device at high angles of attack. The importance of leading edge controls in influencing the entire afterbody is epitomized by the use of spikes. Flow separation spikes in front of blunt bodies may reduce the total drag of the body by effectively streamlining it. Average heat-transfer rates in the separated flow region created by the spike are significantly reduced in laminar flow, although the local heat transfer rate at reattachment may be quite high. Deflectable spikes might be used as control devices because they alter the pressure distribution in the forward region of a body. This technique is also being studied at NASA Ames Research Center. The separated flow region caused by spikes, however, is frequently unsteady, which is a most unsatisfactory control characteristic. If these problems can be worked out, spike controls could become a very effective system for blunt vehicles.

#### Downstream Controls

Frequently control surfaces located downstream of the leading edge may also be used as stabilizing devices. Their effectiveness, however, may be greatly affected by upstream separation of the boundary layer. The inviscid estimate of the pressure rise due to deflecting a control into the local stream is a discontinuous jump in the pressure distribution on the surface at the leading edge of the control. A similar sudden increase in the inviscid pressure distribution occurs at the trailing-edge shock required to recompress the flow over an expansion surface. In the actual flow, the sudden pressure rise may be transmitted upstream through the subsonic portion of the boundary layer. Particularly for hypersonic flow, where shocks are highly swept, and for laminar

boundary layers, which have thicker subsonic portions than turbulent boundary layers, the pressure rise may be felt, and separation may occur, far upstream. Depending upon flow conditions, the boundary layer may be separated over the major portion of the surface thereby greatly influencing the effectiveness of controls located downstream on either compression or expansion surfaces.

Laminar boundary layer separation ahead of a deflected flap on the windward surface of a vehicle spreads the flow-deflection pressure rise over a much larger region than does turbulent separation. The effectiveness of the flap in creating a moment is lessened both by the decrease in the pressure distribution on the flap and by any pressure increase occurring on the surface upstream of the s.g. These effects tend to restrict the desired rearward movement of the center of pressure and reduce the effectiveness of the control. In extreme cases the center of pressure location with laminar separation may be well forward of that for a turbulent boundary layer.

The extent of the separated-flow region, and the pressures imposed on the surface depend on the flap deflection, flow conditions, and nature of the boundary layer ahead of the flap. Reattachment of the separated flow on the flap is usually accompanied by a local heat-transfer rate several times larger than that corresponding to an attached boundary layer; the average heat transfer to the separated flow region, however, is reduced. Similarly, separation affects the pressure distribution on vehicles having flared-skirt-type stabilizing surfaces. Laminar boundary layer flow ahead of small protuberances yields pressure distributions closer to the inviscid predictions than does turbulent flow. A small step on a surface is effectively streamlined by laminar separation far ahead of it, whereas for turbulent separation, a strong shock exists ahead of the step and there is a large increase in the local pressure.

Separation on the leeward side of a vehicle may make shielded controls (i.e., controls which do not "see" the free stream) useless. A few factors combine in making leading-edge separation from the leeward surface of hypersonic vehicles particularly probable. Large angles of attack may be desirable for many hypersonic flight paths. Because high Mach number flows have small limiting expansion angles, much of the upper surface feels only the leakage flow from the boundary layer where the Mach number is lower. The pressure rise due to the strong trailing-edge shock may be propagated far forward through the thick hypersonic boundary layer and

enhances the possibility of leading-edge separation. Another factor enhancing the probability of separation is the likelihood of the boundary layer being laminar with consequently thicker subsonic regions and simultaneously less ability to overcome an adverse pressure gradient than the corresponding turbulent boundary layer. The effectiveness of controls located entirely within the separated flow region, such as trailing-edge flaps or fins, would be nullified. On the other hand, flow separation over notches (cavities) may advantageously be used to control the drag of a hypersonic vehicle; for essentially the same average rate of heat transfer to a hypersonic vehicle, the drag may be increased by an order of magnitude by the employment of notches in the surface of the vehicle. Separation influences both the type and the location of control devices. Spoilers, for example, would be ineffectual on leeward surfaces of hypersonic vehicles even if they were near the leading edge. Positive controls that always "see" the free stream are required.

### Three-Dimensional and Unsteady Flow Effects

Separated-flow regions rarely are purely two-dimensional and usually are unsteady. Although much insight into separation phenomena may be gained using two-dimensional flow analyses, there are important effects that must be considered three-dimensionally. One such effect is the large venting of the separated region in front of a ramp of finite span. The fluid in the separated region, having low velocity and (relatively) high pressure, expands readily into the low-pressure stream at the tip, and the mass balance of the two-dimensional separation is upset. Another case is that associated with the streamwise flow in the corner at the juncture of a fin and the surface of the configuration. A strong vortex may be set up in such a corner with extreme rates of heat transfer associated with the vortical motion. Another important three-dimensional effect is the coupling effect of a control on another surface. The shock wave ahead of a blunt control or ahead of a separated flow region may impinge on a transverse surface. Thus, the deflection of a vertical fin or rudder may cause nonsymmetrical separation on the horizontal surface and create an undesired rolling or pitching moment. Particularly for separation occurring near the point of transition of a laminar to turbulent boundary layer, the point of separation and the associated shock wave may oscillate about some mean position. Large buffeting

loads may be experienced on the surface and on adjoining surfaces of the configuration. Unsteady flow in cavities in the surface of a missile may also cause structural failure. Laminar boundary layer separation with large center-of-pressure shift may be experienced at a small control deflection, while if the deflection is increased and then decreased to its initial value the separation may be turbulent with a far different value of pitching moment because of the different center-of-pressure location. This hysteresis is extremely difficult to predict, and can be quite dangerous.

## CONTROLS FOR HYPERSONIC VEHICLES

The current status of the application of aerodynamic control to hypersonic flight is reviewed in this section. We discuss the existing information on problems of controlling a hypersonic vehicle and of estimating aerodynamic control characteristics, and present, in the Appendix, a synopsis of the experimental information on controls which is available in the literature. The tabulation lists the types of controls tested, the vehicle configurations on which the controls were tested, the test conditions, the type of data obtained and comments concerning special features of the work in each case. This table should serve as an index to the available hypersonic controls data.

### General Discussion

Controls are required to provide maneuvering capability for flight vehicles and can supply the aerodynamic stability and trim necessary to maintain an equilibrium flight trajectory. The most economical and straightforward type of control for a vehicle flying the atmosphere is usually an aerodynamic surface, but the application of aerodynamic control surfaces to hypersonic flight vehicles presents many formidable problems. For flight at very high altitudes aerodynamic controls may be rendered ineffective by low dynamic pressure and very thick boundary layers. At the lower altitudes the deflection of a control can generate separated flow regions over much of the surface of the vehicle and alter the aerodynamic load distribution and stability characteristics.

Standard aerodynamic stability and control problems are greatly aggravated by the large range of angle-of-attack (cf. Ref. 110), high aerodynamic heating rates, and the wide speed range to be encountered by hypersonic flight vehicles. These vehicles also tend to have compact geometries and therefore require high control loads to produce useful moments about the center of gravity. Consequently, the controls tend to become a significant portion of the vehicle's structure and it becomes desirable to build more functions into fewer control surfaces.

The complexity of flow fields about hypervelocity flight vehicles arises from the interplay of many distinctive hypersonic

flow phenomena. The blunt leading edges, which are usually necessitated by aerodynamic heating considerations, lead to strong detached shock waves with their attendant high loads, thick entropy layers, and steep pressure gradients. Much of the surface of the configuration is in close proximity to the highly curved bow shock. Separation and reattachment of the thick boundary layer, secondary shocks, and locally unsteady flow may further complicate analysis of the flow field.

Trailing-edge controls may be rendered useless if they are shielded from the free stream by the basic configuration. Or, they may be subjected to much larger loads than they would experience if they were in the free stream in the absence of the basic configuration. In the latter case, the flow may be compressed through weak oblique shocks generated by the basic configuration, with consequent lower pressure losses and less of an entropy rise, so that the pressure coefficient on the trailing-edge control surface may be much larger than even the stagnation pressure coefficient that would be measured by a total pressure tube in the free stream. Trailing-edge controls may cause the boundary layer to separate far upstream of their hinge lines, thereby affecting the pressure distribution over the vehicle, and may be subjected to local increases in heat-transfer rate by reattachment or unsteadiness of the boundary layer. On the other hand, a control located forward of the c.g. is subjected to severe loads and heating, and changes the flow field over a large part of the vehicle. It can thus adversely effect any downstream controls or stabilizing surfaces.

Available theoretical methods (cf. Refs. 110 through 127) leave much to be desired. The important viscid effects must usually be omitted from the analysis, and furthermore, many methods are based on the supersonic linear theory which, by definition (cf. Ref. 53), fails for hypersonic flows. The flow field about a vehicle may be approximated to varying degrees of accuracy depending upon the complexity of the configuration and the applicability of the methods available. Although the method of characteristics is available, it cannot always be applied. The effects of sweep, incidence, and surface discontinuities force one to rely upon much simpler approximate approaches, such as Newtonian and integral methods, the blast wave analogy, and viscid interaction corrections, which often require experimental verification and the use of empirical data (cf. Refs. 110 and 128 through 169). The best possible estimate of local flow conditions immediately ahead of controls at large deflection angles should be

used in calculations, rather than free stream conditions. High pressures and high heating rates, approaching and even exceeding the body stagnation value, may be experienced on controls (cf. Ref. 170). Heat-transfer calculations for both sharp and blunt leading-edged delta wings can probably be performed adequately using simple strip, streamline divergence, or crossflow theories (Ref. 160).

Most of the theoretical methods currently employed are not completely satisfactory in that they involve the knowledge, "a priori", of some empirical data, and they give no clear indication of the limits of their validity. Experimental data for hypersonic flows are still quite scarce and the data which do exist cannot be extrapolated to differing flow conditions with any degree of certainty. A great deal of the experimental information available, on relatively simple shapes, results from helium tests (cf. Refs. 66 and 160). The use of helium for verification of theoretical methods may improperly eliminate some theories that are more closely applicable to air. The proximity of the entire shock to the body surfaces, boundary layer growth, interaction, real gas effects, and the structure of the entropy layer are all dependent upon the gas used.

### Flaps

Only a small fraction of the available experimental data on trailing-edge flaps are applicable to hypersonic problems. Two-dimensional data on an unswept wing-trailing edge flap configuration, presented in Refs. 171 through 174, cover the Mach number range from 1.62 to 6.9 for angles of attack up to  $10^\circ$  and control deflections from  $-16^\circ$  to  $+16^\circ$ . Section lift, drag, pitching moment, and hinge moment coefficients are presented, as well as chordwise pressure distributions. A more general program to determine control effectiveness, which includes the effects of trailing-edge flaps, is presented in Refs. 175 through 187. This program, although extremely comprehensive in that it investigates the effectiveness of a wide variety of flaps, spoilers, and tip controls individually and in combination on trapezoidal and triangular planform wings, is limited to supersonic Mach numbers between 1.6 and 2.4. The data provided in this program are lift, drag, pitching moment and hinge moment coefficients, as well as pressure distributions on the wing and on the controls. In these

reports only wings and controls are considered; the following discussion deals with those investigations which treat a complete vehicle, usually comprising a wing, body, and vertical fin.

Data on the effectiveness of trailing-edge flaps on various configurations in supersonic flows are presented in Refs. 188 through 195. In particular, Refs. 188 and 194 supply effectiveness information on delta-wing configurations for high angles of attack and large flap deflection angles. Both reports indicate that at high angles of attack and large deflection angles the control effectiveness decreases sharply. The effect of varying the Mach number from supersonic to hypersonic on configurations with different wing planforms and sweep angles can be found in Refs. 196 through 200. Flap effectiveness data at hypersonic Mach numbers, on the various configurations, are presented in Refs. 196 through 204. Experimental investigations of flaps on pyramidal configurations are reported in Refs. 204 and 205. As expected, the longitudinal effectiveness of flaps decreases with increasing dihedral angle while the lateral effectiveness increases with increasing dihedral angle. In Ref. 206 data are presented for a wide variety of wing, wing-body, and wing-body-flap configurations tested over the Mach number range from 2 to 22. This report represents an exploratory effort to determine the usefulness of aerodynamic controls under hypersonic flight conditions.

Aerodynamic heating data for trailing-edge flaps in supersonic streams are presented in Refs. 207 and 208. Heat-transfer data for hypersonic flow over a trailing-edge flap are presented in Ref. 209. These data are limited in their extent and usefulness. The problem of aerodynamic heating of wing-type configurations using aerodynamic controls is an extremely serious one. At present it is virtually unexplored. This lack of information is a serious handicap to the reliable design of hypersonic flight vehicles.

### Fins

Another aerodynamic surface capable of providing maneuvering and stabilizing capabilities is the deflectable fin mounted either fore or aft.

The supersonic characteristics of canard controls, mounted on flight configurations having delta or trapezoidal planform wings, are presented in Refs. 192, 193, and 210 through 214. Some data for hypersonic flows are presented in Ref. 206. These reports indicate that effective canard surfaces can be designed to provide longitudinal control in the supersonic Mach number range. There are not enough data to justify such a conclusion at hypersonic Mach numbers. The heating, separation, and down-wash problems associated with canard surfaces at hypersonic speeds have not been investigated. The usefulness of canard surfaces under hypersonic flight conditions will depend strongly on these effects.

The effect of Mach number variation, from supersonic to hypersonic, on the effectiveness of aft fins, mounted both vertically and horizontally, is presented in Refs. 197 through 199, 206 and 215. Additional empirical data for aft-mounted fins are presented in Refs. 190, 192, 201, 213, and 216 through 223. As may be seen in the Appendix, aerodynamic heating data on fins are presented in Refs. 207 through 209.

The effectiveness of deflected wing tips, tested at supersonic Mach numbers, is presented in Refs. 171, 175 through 177, 179, 182, 185, 186, 188, 189, 224, and 226 through 230. Hypersonic data are presented in Ref. 225. Test conditions and the types of data available in the reports are indicated in the Appendix. The data available indicate that tip controls can be designed to provide aerodynamic control for supersonic flight vehicles. The hypersonic usefulness of these controls cannot be ascertained until the aerodynamic heating problems associated with them are investigated.

#### Others

Control effectiveness information on tip-mounted bodies such as cones, pyramids, and tri-panels, is presented in Refs. 200, 203, and 221. A direct comparison of the control effectiveness of these tip mounted bodies, at a hypersonic Mach number, is made in Ref. 203, while the Mach number dependence of the control effectiveness is shown in Ref. 200.

Other aerodynamic surfaces usable for control and stabilization fall into the general categories of nose spikes, canted noses or drooped leading edges, spoilers, and flares. Many problems arise connected with the use of these more unconventional types of controls. For example, the flow pattern about nose spikes is frequently unstable (Ref. 231). Nose cant enables trimming a vehicle at high angle of attack but, unless the nose is movable, does not provide maneuvering capability (Refs. 194, 200, 203, 204, 205, 216, 217, 231, and 232). The effectiveness of spoilers in decreasing the lift on the upper surface of a wing in transonic and supersonic flows is presented in Refs. 176, 179, 180, 181, 185, 196, 226, 233, and 234. Spoilers on the upper surface of hypersonic vehicles, at angle of attack, would be operating in a very low-pressure region, and would be useless. The use of spoilers on the compression surface to produce additional force, remains to be adequately investigated. Flares are basically stabilizing devices, although movable flares, theoretically, could be used for control (Ref. 216) if mechanical problems could be overcome.

The experimental information available for hypersonic flows is generally in the form of force data on particular configurations. The most important point to remember in a survey of these data is the tremendous number of geometric variations characteristic of the different approaches to design of hypersonic flight vehicles. The probability of finding tests on a specific practical geometry in a given flow regime is indeed small, and attempts to provide a catalogue of all control problems of possible interest would be grossly inefficient in terms of the cost of the tests. We feel that the only reasonable approach to this problem is a coupling of: 1) an increased theoretical understanding of fundamental flow phenomena, 2) experiments on simplified geometries wherein separate effects can be isolated, 3) experiments on typical types of interactions among different flow phenomena brought about by superposition of geometries, 4) a catalogue of those experiments which have been conducted for other purposes, and 5) final testing of a design which is created using the information in items 1) through 4). Our purpose in this contract is to provide some of the information needed to apply this approach.

## CONCLUSIONS AND RECOMMENDATIONS

This section contains a brief statement of the present status of hypersonic flow separation and control problems. Detailed descriptions of the phenomena and results of investigations are presented in the preceding sections. General conclusions, based on the knowledge accumulated for separation and control, are made before recommending particular areas of the problems where much further work is required.

Our knowledge of separation is almost completely limited to flows below hypersonic speeds. Data on hypersonic flow separation problems are only beginning to appear, and most of the existing theories do not include such important hypersonic phenomena as the nonlinearity of the flow equations and the effects of variations in fluid properties at very high temperatures (real gas effects). We have tried to present what information is available, because theories for hypersonic flow separation will most probably be constructed along the same lines as those for supersonic cases, and the qualitative nature of the flows in the two cases will be similar.

The shapes of the pressure distributions over laminar and turbulent separated flow regions, and the effects of pressure increases on laminar and turbulent boundary layers are qualitatively known on windward surfaces. The location of transition of the boundary layer from laminar to turbulent flow substantially affects separation but is quite difficult to predict. Lengthy theoretical methods are available for separated laminar boundary layers, but there are serious limitations on their applicability and validity. Empirical methods are available for both laminar and turbulent separated boundary layers. The methods may be used to predict regions of separated flow and the resulting pressure distributions. Separated flows over leeward surfaces may be of much greater extent and are less amenable to theoretical methods, but also are usually less important because of the low pressures on leeward surfaces at hypersonic speeds. Temperature and heat-transfer effects on laminar boundary layers over simple shapes are understood only qualitatively, and the effects are not even qualitatively understood for turbulent boundary layers.

Analyses of boundary layer separation effects on the characteristics of various types of aerodynamic controls are complicated by three-dimensional effects and interaction between configuration components. The existing data on the relative importance of the various parameters is sparse, and the effects of different configurations on control characteristics have not been compared. It is generally agreed that a control should not be shielded from the free stream and that an empirical approach is still required for each new control configuration. Available control data are indicated in the Appendix.

Although additional work in practically all areas of hypersonic flow separation is required, we believe the following need special attention:

The importance of violations of the Prandtl boundary layer assumptions should be evaluated, and solutions of boundary layer equations including additional terms important for hypersonic flows should be developed, even if only approximately.

The better theoretical and semiempirical methods for supersonic separated flows should be extended to include hypersonic phenomena of nonlinearity, real gas effects, stronger shock interactions, and large transport property variations.

Additional experimental research is required to understand better the relationship between boundary layer transition and separation.

Both theoretical and experimental research should be accomplished to determine the influence of wall temperature on separation and the effects of separation on heat-transfer rates.

A systematic investigation of three-dimensional effects on separation, such as the effect of finite span on separation ahead of a compression flap, should be conducted.

The stability of separated flows should be investigated; the conditions under which oscillations occur, their

frequency and amplitude characteristics, and their effect on heat transfer should be determined.

The present knowledge of hypersonic control surface characteristics is mainly deficient in its lack of generality. It is now necessary to test a complete geometry in order to be able to predict how the control forces will behave. We therefore recommend an increased emphasis on verification of analytical design methods, with special emphasis on the interaction between a control surface and the flow generated by neighboring configuration components. Emphasis in experiments should be on determining, individually, the effects of increased Mach number, three-dimensional effects, and heat-transfer characteristics.

## REFERENCES

- 1 Schlichting, H., Boundary Layer Theory, McGraw-Hill Book Co., New York, 1955, pp. 297-307.
- 2 Modern Developments in Fluid Dynamics - High Speed Flow, Edited by L. Howarth, Vol. I, Oxford University Press, 1953.
- 3 Chapman, D.R., Kuehn, D., and Larson, H.K., Investigation of Separated Flows in Supersonic and Transonic Streams with Emphasis on the Effect of Transition, NACA TR 1356, 1958, (Supersedes NACA TN 3869).
- 4 Sterrett, J.R., and Emery, J.C., Extension of Boundary-Layer-Separation Criteria To A Mach Number of 6.5 By Utilizing Flat Plates With Forward-Facing Steps, NASA TN D-618, December 1960.
- 5 Hammitt, A.G., The Interaction of Shock Waves and Turbulent Boundary Layers, JAS, Vol. 25, No. 6, June 1958.
- 6 Lange, R.H., Present Status of Information Relative to the Prediction of Shock-Induced Boundary-Layer Separation, NACA TN 3065, February 1954.
- 7 Reshotko, E., and Tucker, M., Effect of a Discontinuity On Turbulent Boundary-Layer-Thickness Parameters With Application to Shock-Induced Separation, NACA TN 3454, May 1955.
- 8 Drougge, G., An Experimental Investigation of the Influence of Strong Adverse Pressure Gradients on Turbulent Boundary Layers at Supersonic Speeds, Aero. Res. Inst. of Sweden, Rep. No. 46, 1953.
- 9 Love, E.S., Pressure Rise Associated With Shock-Induced Boundary-Layer Separation, NACA TN 3601, December 1955.
- 10 Shapiro, A.H., The Dynamics and Thermodynamics of Compressible Fluid Flow, Vol. 11, The Ronald Press Co., New York, 1954, pp. 1138-1159.

## REFERENCES (Cont.)

- 11 Schuh, H., On Determining Turbulent Boundary-Layer Separation in Incompressible and Compressible Flow, JAS, Vol. 22, No. 5, May 1955.
- 12 Donaldson, C. duP., and Lange, R.H., Study of the Pressure Rise Across Shock Waves Required to Separate Laminar and Turbulent Boundary Layers, NACA TN 2770, September 1952.
- 13 Chapman, D.R., A Theoretical Analysis of Heat Transfer in Regions of Separated Flows, NACA TN 3792, October 1956.
- 14 Larson, H.K., Heat Transfer in Separated Flows, JAS, Vol. 26, No. 11, November 1959, (supersedes IAS Preprint 59-37).
- 15 Cohen, C.B., and Reshotko, E., Similiar Solutions For the Compressible Laminar Boundary Layer With Heat Transfer and Pressure Gradient, NACA TR 1293, 1956.
- 16 Cohen, C.B., and Reshotko, E., The Compressible Laminar Boundary Layer With Heat Transfer and Arbitrary Pressure Gradient, NACA TR 1294, 1956.
- 17 Gadd, G.E., The Numerical Integration of the Laminar Compressible Boundary Layer Equations, With Special Reference to the Position of Separation When the Wall is Cooled, Aero. Res. Council., Rep. 15,101, FM 1771, August 1952.
- 18 Gadd, G.E., A Theoretical Investigation of the Effects of Mach Number, Reynolds Number, Wall Temperature and Surface Curvature On Laminar Separation in Supersonic Flow, Aero. Res. Council., Rep. 18,494, June 1956.
- 19 Gadd, G.E., A Review of Theoretical Work Relevant to the Problem of Heat Transfer Effects on Laminar Separation, Aero. Res. Council., Rep. 18,495, June 1956.
- 20 Illingworth, C.R., The Effect of Heat Transfer On the Separation of a Compressible Laminar Boundary Layer, Quart. F. Mech. Appl. Math. 7, 8, 1954.

## REFERENCES (Cont.)

- 21 Morduchow, M., and Grape, R.G., Separation, Stability, and Other Properties of Compressible Laminar Boundary Layer With Pressure Gradient and Heat Transfer, NACA TN 3296, May 1955.
- 22 Sogin, H.H., Burkhard, K., and Richardson, P.D., Heat Transfer In Separated Flows, Pt. I - Preliminary Experiments on Heat Transfer from an Infinite Fluff (sic Bluff) Plate to an Air Stream, Pt. II - Survey on Separated Flows, With Special Reference to Heat Transfer, Aeronautical Research Lab., ARL-4, January 1961.
- 23 Kuo, Y.H., Dissociation Effects in Hypersonic Viscous Flows, JAS, Vol. 24, No. 5, May 1957.
- 24 Gadd, G.E., An Experimental Investigation of Heat Transfer Effects on Boundary Layer Separation in Supersonic Flow, Jour. of Fluid Mechanics, Vol. 2, Part 2, March 1957.
- 25 Gadd, G.E., and Holder, D.W., The Behaviour of Supersonic Boundary Layers in the Presence of Shock Waves, IAS Paper No. 59-138, October 5-7, 1959.
- 26 Gadd, G.E., Boundary Layer Separation in the Presence of Heat Transfer, AGARD Report 280, (NASA Listing N-100,743), April 1960.
- 27 Crocco, L., and Lees, L., A Mixing Theory For the Interaction Between Dissipative Flows and Nearly Isentropic Streams, JAS, Vol. 19, No. 10, October 1952.
- 28 Thwaites, B., Approximate Calculation of the Laminar Boundary Layer, Aeronautical Quarterly, Vol. I, May 1949 - February 1950.
- 29 Martellucci, A., and Libby, P.A., Heat Transfer Due to the Interaction Between A Swept Planar Shock Wave and a Laminar Boundary Layer, Gen'l. Appl. Sci. Lab. Tech. Rep. 247, 1961.
- 30 Cheng, Sin-I, and Bray, K.N.C., On the Mixing Theory of Crocco & Lees and its Application to Shock Wave-Laminar Boundary Layer Interaction - Part I., Princeton University Aeronautical Engineering Report 376, March 1957.

### REFERENCES (Cont.)

- 31 Glick, H.S., Modified Crocco-Lees Mixing Theory for Supersonic Separated and Reattaching Flow, GALCIT Memo. No. 53, Pasadena, California, May 1960.
- 32 Stewartson, K., Correlated Incompressible and Compressible Boundary Layers, Proc. Roy. Soc. (A), Vol. 200, p. 84: 1949.
- 33 Crocco, L., Considerations on The Shock-Boundary Layer Interaction, Proceedings on the Conference on High-Speed Aeronautics, held at the Polytechnic Institute of Brooklyn, January 20-22, 1955.
- 34 Cheng, Sin-I., and Chang, I.D., On the Mixing Theory of Crocco & Lees and its Application to Shock Wave-Laminar Boundary Layer Interaction - Part II, Princeton University Aeronautical Engineering Report 376, November 1957.
- 35 Hakkinen, R.J., Greber, I., Trilling, L., and Abarbanel, S.S., The Interaction of an Oblique Shock Wave with a Laminar Boundary Layer, NASA Memo. 2-18-59 W, March 1959.
- 36 Howarth, L., On the Solution of the Laminar Boundary Layer Equations, Proceedings of the Royal Society, Series A, Vol. 164, January - February 1938.
- 37 Hartree, D.R., A Solution of the Boundary Layer Equation for Schubauer's Observed Pressure Distribution for an Elliptic Cylinder, Aero. Res. Council., Rep. 3966, 1939.
- 38 Schubauer, G.B., Air Flow in a Separating Laminar Boundary Layer, NACA TR 527, 1935.
- 39 Bray, K.N.C., Gadd, G.E., and Woodger, Some Calculations by the Crocco-Lees and Other Methods of Interaction Between Shock Waves and Laminar B.L.'s Including Effects of High Temperature and Suction, Aero. Res. Council., Rep. 21,834, FM 2937, April 1960.
- 40 Stewartson, K., Further Solutions of the Falkner-Skan Equation, Proc. Camb. Phil. Soc., Vol. 50, p. 454, 1954.

REFERENCES (Cont.)

- 41 Mager, A., Prediction of Shock-Induced Turbulent Boundary-Layer Separation, JAS, Vol. 22, No. 3, March 1955.
- 42 Mager, A., On the Model of the Free, Shock-Separated, Turbulent Boundary Layer, JAS, Vol. 23, No. 2, February 1956.
- 43 Mager, A., Transformation of the Compressible Turbulent Boundary Layer, JAS, Vol. 25, No. 5, May 1958.
- 44 Culick, F., and Hill, J.A., A Turbulent Analog of the Stewartson-illingworth Transformation, JAS, Vol. 25, No. 4, April 1958.
- 45 Tyler, R.D., and Shapiro, A.H., Pressure Rise Required for Separation in Interaction Between Turbulent Layer and Shock Wave, JAS, Vol. 20, No. 12, December 1953.
- 46 Bogdonoff, S.M., and Kepler, C.E., Separation of a Supersonic Turbulent Boundary Layer, JAS, Vol. 22, No. 6, June 1955.
- 47 Gadd, G.E., Interactions Between Normal Shock Waves and Turbulent Boundary Layers, Aero. Res. Council., Rep. 22,559, FM 3051, February 1961.
- 48 Honda, M., A Theoretical Investigation of the Interaction Between Shock Waves and Boundary Layers, JAS, Vol. 25, No. 11, November 1958.
- 49 Honda, M., A Theoretical Investigation of the Interaction Between Shock Waves and Boundary Layers, Erratum, JAS, Vol. 27, No. 1, January 1960.
- 50 Gadd, G.E., A Simple Theory for Interactions Between Shock Waves and Entirely Laminar Boundary Layers, JAS, Vol. 23, No. 3, March 1956.
- 51 Gadd, G.E., A Theoretical Investigation of Laminar Separation in Supersonic Flow, JAS, Vol. 24, No. 10, October 1957.

## REFERENCES (Cont.)

- 52 Picken, J., Free Flight Measurements of Pressure and Heat Transfer in Regions of Separated and Reattached Flow at Mach Numbers up to 4, Report AERO-2643, September 1960 (Confidential - M.H.A.).
- 53 Kaufman, L.G., and Scheuing, R.A., An Introduction to Hypersonics, Grumman Research Department Report RE-82, ASTIA AD 243 027, 2nd ed. August 1960.
- 54 Poots, G., A Solution of the Compressible Laminar Boundary Layer Equations with Heat Transfer and Adverse Pressure Gradient, Quart. Jour. Mech. Appl. Math., Vol. 13, pp. 57-84, 1960.
- 55 Seban, R.A., Emery, A., and Levy, A., Heat Transfer to Separated and Reattached Subsonic Turbulent Flows Obtained Downstream of a Surface Step, JAS, Vol. 26, No. 12, December 1959.
- 56 Sprinks, T., A Review of Work Relevant to the Study of Heat Transfer in Hypersonic Separated Flows, University of Southampton, Abstract U.S.A.A. No. 138.
- 57 Cohen, N.B., Correlation Formulas and Tables of Density and some Transport Properties of Equilibrium Dissociating Air for use in Solutions of the Boundary-Layer Equations, NASA TN D-194, February 1960.
- 58 Budesca, J.G., Hypersonic Inlet Location Study, Grumman Research Department Memorandum RM-187, June 1961.
- 59 Vas, I.E., A Detailed Study of the Interaction of a 14° Shock Wave with a Turbulent Boundary Layer at M = 2.9, AFOSR TN 55-201, April 1955.
- 60 Vas, I.E., and Bogdonoff, S.M., Interaction of a Shock Wave with a Turbulent Boundary Layer at M = 3.85, Princeton University Report No. 294, AFOSR TN 55-199, April 1955.
- 61 Spagnolo, F.A., and Kaufman, L.G., Tables of Oblique Shock Functions for an Ideal Diatomic Gas, Grumman Research Department Memorandum RM-180, October 1960.

## REFERENCES (Cont.)

- 62 Kuehn, D.M., Experimental Investigation of the Pressure Rise Required for the Incipient Separation of Turbulent Boundary Layers in Two-Dimensional Supersonic Flow, NASA Memo 1-21-59A, February 1959.
- 63 Greber, I., Shock-Wave Laminar Boundary-Layer Interaction On a Convex Wall, Mass. Inst. of Tech., NASA TN D-512, October 1960.
- 64 Love, E.S., On the Effect of Reynolds Number Upon the Peak Pressure-Rise Coefficient Associated with the Separation of a Turbulent Boundary Layer in Supersonic Flow, JAS, Vol. 22, No. 5, May 1955.
- 65 Lankford, J.L., The Effect of Heat Transfer on the Separation of Laminar Flow Over Axisymmetric Compression Surfaces in Hypersonic Flow, NOL Preprint, October 1961.
- 66 Bogdonoff, S.M., and Vas, I.E., A Study of Hypersonic Wings and Controls, IAS, Paper No. 59-112, June 1959.
- 67 Bloom, M.H., On Moderately Separated Viscous Flows, JAS, Vol. 23, No. 4, April 1961.
- 68 Lessen, M., On the Hydrodynamic Stability of Curved Compressible Flows, IAS Preprint 312, January 1958.
- 69 Lees, L., Note on the Stabilizing Effect of Centrifugal Forces on the Laminar Boundary Layer Over Convex Surfaces, JAS, Vol. 25, No. 6, June 1958.
- 70 Murthy, Amanda, K.R., and Hammitt, A.G., Investigation of the Interaction of a Turbulent Boundary Layer with Prandtl-Meyer Expansion Fans at  $M = 1.83$ , Princeton Univ., Rep. 434, August 1958.
- 71 Beheim, M.A., Flow in the Base Region of Axisymmetric and Two-Dimensional Configurations, NASA TR R-77, 1960.

### REFERENCES (Cont.)

- 72 Love, E.S., Base Pressure at Supersonic Speeds On Two-Dimensional Airfoils and On Bodies of Revolution with and without Fins having Turbulent Boundary Layers, NACA TN 3819, January 1957.
- 73 Ferrari, C., Airfoil Pressures at Supersonic Speeds Under Separated Flow Conditions, Applied Physics Lab., The Johns Hopkins University, August 1957.
- 74 Fraser, R.P., Eisenklam, P., and Wilkie, D., Investigation of Supersonic Flow Separation in Nozzles, Journal Mechanical Engineering Science, Vol. 1, No. 3, 1959.
- 75 Lochtenberg, B.H., Transition in a Separated Laminar Boundary Layer, JAS, Vol. 27, No. 2, February 1960.
- 76 Kline, S., Some New Conceptions of the Mechanism of Stall in Turbulent Boundary Layers, JAS, Vol. 24, No. 6, June 1957.
- 77 Sears, W.R., Boundary Layers in Three-Dimensional Flow, Appl. Mech. Reviews Vol. 7, No. 7, July 1954.
- 78 Moore, F.K., Advances in Applied Mechanics, Vol. IV, p. 202, Academic Press, 1956.
- 79 Oman, R.A., The Three-Dimensional Laminar Boundary Layer Along a Corner, Sc.D. Thesis, M.I.T., ASTIA AD 211216, June 1959.
- 80 Randall, R.E., Bell, D.R., and Burk, J. L., Pressure Distribution Tests of Several Sharp Leading Edge Wings, Bodies, and Body-Wing Combinations at Mach 5 and 8, AEDC TN 60-173, 1960.
- 81 Stalker, R.J., The Pressure Rise at Shock-Induced Turbulent Boundary-Layer Separation in Three-Dimensional Supersonic Flow, JAS, Vol. 24, No. 7, July 1957.
- 82 Stalker, R.J., Sweepback Effects in Turbulent Boundary-Layer Shock-Wave Interaction, JAS, Vol. 27, No. 5, May 1960.

REFERENCES (Cont.)

- 83 Cooke, J.C., and Hall, M.G., Boundary Layers in Three Dimensions, RAE Rep. No. 2635, AD 235 751, 1957.
- 84 Cooke, J.C., A Calculation Method for Three-Dimensional Turbulent Boundary Layers, Aero. Res. Council., R. & M. No. 3199, 1961. Supersedes RAE TN Aero 2576, October 1958.
- 85 Bloom, M.H., and Rubin, S., High Speed Viscous Corner Flow, JAS., Vol. 28, No. 2, February 1961.
- 86 Stewartson, K., and Howarth, L., On the Flow Past a Quarter-Infinite Plate Using Oseen's Equations, Journal of Fluid Mechanics, Vol. 7, Part I, January 1960.
- 87 Trilling, L., Oscillating Shock Boundary-Layer Interaction, JAS, Vol. 25, No. 5, May 1958.
- 88 Kaufman, L.G., and Morduchow, M., On the Stability of One-Dimensional Viscous Flows: Sound Waves and Shock Waves, WADC TR 59-355, August 1959.
- 89 Fiszdon, W., and Mollo-Christensen, E., An Experiment on Oscillatory Shock-Wave Boundary-Layer Interaction, JAS, Vol. 27, No. 1, January 1960.
- 90 Charwat, A.F., Roos, J.N., Dewey, F.C., and Hitz, J.A., An Investigation of Separated Flows - Part I, JAS, Vol. 28, No. 6, June 1961.
- 91 Charwat, A.F., Roos, J.N., Dewey, F.C., and Hitz, J.A., An Investigation of Separated Flows - Part II, JAS, Vol. 28, No. 7, July 1961.
- 92 Larson, H.H., and Keating, S.J., Transition Reynolds Numbers of Separated Flows at Supersonic Speeds, NASA TN D-349, December 1960.
- 93 Donaldson, J.C., and Bell, D.R., Sound and Pressure Measurements in Cavities on a Body of Revolution at Supersonic Speeds, AEDC TN 60-233, January 1961.
- 94 McDearmon, R.W., Investigation of the Flow in a Rectangular Cavity in a Flat Plate at a Mach Number of 3.55, NASA TN D-523, September 1960.

REFERENCES (Cont.)

- 95 Stalder, J.R. and Nielsen, H.V., Heat Transfer from a Hemisphere-Cylinder Equipped with Flow-Separation Spikes, NACA TN 3287, September 1954.
- 96 Bogdonoff, S.M., and Vas, I.E., Preliminary Investigations of Spiked Bodies at Hypersonic Speeds, JAS, Vol. 26, No. 2, February 1959.
- 97 Bogdonoff, S.M., and Vas, I.E., Hypersonic Separated Flows, IAS Paper 59-139, October 1959.
- 98 Lynes, L.L., and Schaaf, S.A., Some Preliminary Results in Separated Flow Aerodynamics, University of Calif. Tech. Rep. HE-150-178, February 1960.
- 99 Canning, T.N., Investigation of the Lift, Center of Pressure, and Drag of a Projectile at a Mach Number of 8.6 and a Reynolds Number of 17 Million, NACA RM A54H23a, November 1954 (Confidential).
- 100 Becker, J.W., and Korycinski, P.F., Heat Transfer and Pressure Distribution at a Mach Number of 6.8 on Bodies with Conical Flares and Extensive Flow Separation, NACA RM L56F22, August 1956 (Confidential).
- 101 Sisson, J.M., Preliminary Study of Floating-Wire Boundary Layer Trips for Preventing Flow Separation in the Low Reynolds Number - High Mach Number Regime, Marshall Space Flight Center, Huntsville, Alabama, Report No. MTP-Aero-61-20, March 1961.
- 102 Picken, J., Free-Flight Measurements of Pressure and Heat Transfer in Regions of Separated and Reattached Flow at Mach Numbers Up to 4, RAE TN Aero 2643, September 1960, (Ask NASA for N-92556).
- 103 Stephens, E.W., Afterbody Heating Data Obtained from an Atlas-Boosted Mercury Configuration in a Free Body Reentry, NASA TM X-493, August 1961, (Confidential).

REFERENCES (Cont.)

- 104 Weston, K.C., and Swanson, J.E., A Compilation of Wind-Tunnel Heat-Transfer Measurements on the Afterbody of the Project Mercury Capsule Reentry Configuration, NASA TM X-495, August 1961, (Confidential).
- 105 Liepmann, H.W., Roshko, A., and Dhawan, S., On Reflection of Shock Waves from Boundary Layers, NACA Rep. 1100, 1952.
- 106 Physical Measurements in Gas Dynamics and Combustion, edited by: Ladenbury, R.W., Lewis, B., Pease, R.N., and Taylor, H.S., Vol. IX of High Speed Aerodynamics and Jet Propulsion, Princeton University Press, Princeton, New Jersey, p. 215, 1954.
- 107 Liepmann, H.W., and Roshko, A., Elements of Gasdynamics, John Wiley & Sons, Inc., New York, 1957.
- 108 Pearcey, H.H., The Indication of Boundary Layer Transition on Aerofoils in the N.P.L. 20 inch by 3 inch High Speed Wind Tunnel, British A.R.C. 11, 991, December 1948.
- 109 Van Driest, E.R., Turbulent Boundary Layer in Compressible Fluids, JAS, Vol. 18, No. 3, March 1951.
- 110 Phillips, W.H., Research on Blunt-Faced Entry Configurations at Angles of Attack Between 60° and 90°, USAF-NASA Joint Conference, April 1960.
- 111 Multhopp, H., On the Design of Hypersonic Aircraft, IAS Paper No. 61-17.
- 112 Lagerstrom, P.A., and Graham, M.E., Linearized Theory of Supersonic Control Surfaces, JAS, Vol. 16, No. 1, January 1949.
- 113 Malvestuto, F.S., Margoles, K., and Rebner, H.S., Theoretical Lift and Damping in Roll at Supersonic Speeds of Thin Swept-back Tapered Wings with Streamwise Tips, Subsonic Leading Edge, and Supersonic Trailing Edges, NACA TR 970, 1950.
- 114 Tucker, W.A., and Nelson, R.A., Theoretical Characteristics in Supersonic Flow of Constant Chord Partial-Span Control Surfaces on Rectangular Wings having Finite Thickness, NACA TN 1708, September 1948.

REFERENCES (Cont.)

- 115 Ivey, H.R., Notes on the Theoretical Characteristics of Two-Dimensional Supersonic Airfoils, NACA TN 1179, January 1947.
- 116 Morrisette, R.R., and Oborny, L.F., Theoretical Characteristics of Two-Dimensional Supersonic Control Surfaces, NACA TN 2486, October 1951.
- 117 Tucker, W.A., and Nelson, R.L., Theoretical Characteristics in Supersonic Flow of Two Types of Control Surfaces on Triangular Wings, NACA TR 939, 1949.
- 118 Kainer, J. and King, M., The Theoretical Characteristics of Triangular-Tip Control Surfaces at Supersonic Speeds. Mach Lines Behind Trailing Edges, NACA TN 2715, July 1952.
- 119 Goin, K.L., Equations and Charts for the Rapid Estimation of Hinge-Moment and Effectiveness Parameters for Trailing Edge Controls having Leading and Trailing Edges Swept Ahead of the Mach Lines, NACA TR 1041, 1951.
- 120 Ivey, H.R., Stickle, C.W., and Schuettler, A., Charts for Determining the Characteristics of Sharpnosed Airfoils in Two-Dimensional Flow at Supersonic Speeds, NACA TN 1143, January 1947.
- 121 Dugan, D.W., Estimation of Static Longitudinal Stability of Aircraft Configurations at High Mach Numbers and at Angles of Attack Between 0° and -180°, NASA Memo #1-17-59A, March 1959.
- 122 Freck, C.W., Application of the Linearized Theory of Supersonic Flow to the Estimation of Control-Surface Characteristics, NACA TN 1554, March 1948.
- 123 Love, E.S., The Use of Cones as Stabilizing and Control Surfaces at Hypersonic Speeds, NACA RM L57F14, August 1957.
- 124 Bobbett, P.J., Tables for the Rapid Estimation of Downwash and Sidewash Behind Wings Performing Various Motions at Supersonic Speeds, NASA Memo 2-20-59L, May 1959.
- 125 Yates, E.C., Theoretical Analysis of Linked Leading-Edge and Trailing-Edge Flap-Type Controls at Supersonic Speeds, NACA TN 3617, March 1956.

REFERENCES (Cont.)

- 126 Goin, K.L., Theoretical Analyses to Determine Unbalanced Trailing-Edge Controls Having Minimum Hinge Moments Due to Deflection at Supersonic Speeds, NACA TN 3471, August 1955.
- 127 Klunker, E.B., and Harder, K.C., General Solutions for Flow Past Slender Cambered Wings with Swept Trailing Edges and Calculation of Additional Loading Due to Control Surfaces, NACA TN 4242, May 1958.
- 128 Hayes, W.D., and Probst, R.F., Hypersonic Flow Theory, Academic Press, 1959.
- 129 Freeman, N.C., On the Theory of Hypersonic Flow Past Plane and Axially Symmetric Bluff Bodies, Journal of Fluid Mechanics, Vol. 1, Part 4, 1956.
- 130 Freeman, N.C., On the Newtonian Theory of Hypersonic Flow at Large Distances from Bluff Hypersonics Conference, Preprint No. 1981-61, August 1961.
- 131 Yakura, J.K., A Theory of Entropy Layers and Nose Bluntness in Hypersonic Flow, ARS International Hypersonics Conference, Preprint No. 1983-61, August 1961.
- 132 Taylor, G.I., The Formation of a Blast Wave by a Very Intense Explosion, Part I Theoretical Discussion, Proc. Roy. Soc. (London), Ser. A, Vol. 201, No. 1065, March 22, 1950.
- 133 Lin, S.C., Cylindrical Shock Waves Produced by Instantaneous Energy Release, Journal of Applied Physics, Vol. 25, No. 1, January 1954.
- 134 Sakurai, A., On the Propagation and Structure of the Blast Wave, I, J. Phys. Soc. Japan, Vol. 8, 1953, pp. 662-669.
- 135 Sakurai, A., On the Propagation and Structure of the Blast Wave, II, J. Phys. Soc. Japan, Vol. 9, 1954, pp. 256-266.
- 136 Cheng, H.K., and Pallone, A.J., Inviscid Leading Edge Effecting Hypersonic Flow, JAS, Vol. 23, No. 7, July 1956.

### REFERENCES (Cont.)

- 137 Lees, L., and Kubota, T., Inviscid Hypersonic Flow Over Blunt-Nosed Slender Bodies, JAS, Vol. 24, No. 3, March 1957.
- 138 Kubota, T., Inviscid Hypersonic Flow over Blunt-Nosed Slender Bodies, Heat Transfer and Fluid Mechanics Institute, June 19-21, 1957, California Institute of Technology, Pasadena, Calif. Also, GALCIT Hypersonic Research Project Memorandum 40, June 25, 1957.
- 139 Swigart, R.J., Third Order Blast Wave Theory and Its Application to Hypersonic Flow Past Blunt-Nosed Cylinders, Journal of Fluid Mechanics, Vol. 9, Part 4, December 1960.
- 140 Swigart, R.S., On the Shock Shape and Pressure Distribution About Blunt-Nosed Cylinders Using Blast-Wave Theory, JAS, Vol. 28, No. 10, October 1961.
- 141 Mirels, H., Approximate Analytical Solutions for Hypersonic Flow Over Slender Power Law Bodies, NASA Tech. Rep. R-15, 1959.
- 142 Van Hise, V., Analytic Study of Induced Pressure on Long Bodies of Revolution with Varying Nose Bluntness at Hypersonic Speeds, NASA Tech. Rep. R-73.
- 143 Feldman, S., Numerical Comparison Between Exact and Approximate Theories of Hypersonic Inviscid Flow Past Slender Blunt-Nosed Bodies, ARS Journal, Vol. 30, No. 5, May 1960.
- 144 Baradell, D.L., and Bertram, M.H., The Blunt Plate in Hypersonic Flow, NASA Tech. Note D-408, October 1960.
- 145 Vaglio-Laurin, R., and Trella, M., A Study of Flow Fields About Some Typical Blunt-Nosed Slender Bodies, Polytechnic Institute of Brooklyn, PIBAL Rep. No. 623, December 1960.
- 146 Capiiaux, R., and Karchmar, L., Flow Past Slender Blunt Bodies - A Review and Extension, National IAS/ARS Joint Meeting, June 1961, Paper No. 61-210-1904.

REFERENCES (Cont.)

- 147 Ferri, A., and Libby, P.A., Note on an Interaction Between the Boundary Layer and the Inviscid Flow, JAS, Vol. 21, February 1954.
- 148 Lees, L., Influence of the Leading-Edge Shock Wave on the Laminar Boundary Layer at Hypersonic Speeds, JAS, Vol. 23, June 1956.
- 149 Lees, L., Recent Developments in Hypersonic Flow, Jet Propulsion, November 1957.
- 150 Bertram, M.H., and Henderson, A., Effects of Boundary-Layer Displacement and Leading-Edge Bluntness on Pressure Distribution, Skin Friction, and Heat Transfer of Bodies at Hypersonic Speeds, NACA TN 4301, July 1958.
- 151 Bertram, M.H., Boundary-Layer Displacement Effects In Air at Mach Numbers of 6.8 and 9.6, NASA Tech. Rep. R-22, 1959.
- 152 Creager, M.O., The Effect of Leading-Edge Sweep and Surface Inclination on the Hypersonic Flow Field Over a Blunt Flat Plate, NASA Memo 12-26-58A, January 1959.
- 153 Creager, M.O., Surface Pressure Distribution at Hypersonic Speeds for Blunt Delta Wings at Angle of Attack, NASA Memo 5-12-59A, May 1959.
- 154 Creager, M.O., High-Altitude Hypervelocity Flow Over Swept Blunt Glider Wings, IAS No. 59-113, Presented at the IAS National Summer Meeting, June 16-19, 1959.
- 155 Creager, M.O., An Approximate Method for Calculating Surface Pressures on Curved Profile Blunt Plates in Hypersonic Flow, NASA TN D-71, September 1959.
- 156 Burke, A.F., Blunt-Nose and Real Fluid Effects in Hypersonic Aerodynamics, IAS No. 59-114, Presented at the IAS Summer Meeting, June 16-19, 1959.
- 157 Moore, F.K., and Cheng, H.K., The Hypersonic Aerodynamics of Slender and Lifting Configurations, IAS No. 59-125, Presented at the IAS National Summer Meeting, June 16-19, 1959.

### REFERENCES (Cont.)

- 158 Hayes, W.D., and Probstein, R.F., Viscous Hypersonic Similitude, JAS, Vol. 26, No. 12, p. 815, December 1959.
- 159 Mueller, J.N., Close, W.H., and Henderson, A., An Investigation of Induced-Pressure Phenomena on Axially Symmetric, Flow-Aligned, Cylindrical Models Equipped with Different Nose Shapes at Free-Stream Mach Numbers From 15.6 to 21 in Helium, NASA TN D-373, May 1960.
- 160 Bertram, M.H., and Blackstock, T.A., Some Simple Solutions to the Problem of Predicting Boundary-Layer Self-Induced Pressures, NASA TN D-798, April 1961.
- 161 Cheng, H.K., Hall, G.J., Golian, T.C., and Hertzberg, A., Boundary-Layer Displacement and Leading-Edge Bluntness Effects in High-Temperature Hypersonic Flow, JAS, Vol. 28, No. 5, May 1961.
- 162 Bertram, M.H., and Henderson, A., Recent Hypersonic Studies of Wings and Bodies, ARS Journal, Vol. 31, No. 8, August 1961.
- 163 Maslen, S.H., and Moeckel, W.E., Inviscid Hypersonic Flow Past Blunt Bodies, JAS, Vol. 24, No. 9, September 1957.
- 164 Vaglio-Laurin, R., and Ferri, A., Theoretical Investigation of the Flow Field About Blunt-Nosed Bodies in Supersonic Flight, JAS, Vol. 25, No. 12, December 1958.
- 165 Traugott, S.C., An Approximate Solution of the Direct Supersonic Blunt-Body Problem for Arbitrary Axisymmetric Shapes, JAS, Vol. 27, No. 5, May 1960.
- 166 Van Dyke, M.D., and Gordon, H.D., Supersonic Flow Past a Family of Blunt Axisymmetric Bodies, NASA Tech. Rep. R-1, 1959.
- 167 Vaglio-Laurin, R., On the PLK Method and the Supersonic Blunt Body Problem, IAS Paper No. 61-22, January 1961.

REFERENCES (Cont.)

- 163 Bertram, M.H., Feller, W.V., and Dunavant, J.C., Flow Fields, Pressure Distributions, and Heat Transfer for Delta Wings at Hypersonic Speeds, USAF-NASA Joint Conference, April 1960.
- 169 Seiff, A., and Whiting, E., The Effect of the Bow Shock Wave on the Stability of Blunt-Nosed Slender Bodies, USAF-NASA Joint Conference, April 1960.
- 170 Reller, J.O., and Seegmiller, H.L., Convective Heat Transfer to a Blunt Lifting Body, USAF-NASA Joint Conference, April 1960.
- 171 Czarnecki, K.R., and Mueller, J.N., Investigation at Mach Number 1.62 of the Pressure Distribution Over a Rectangular Wing with Symmetrical Circular-Arc Section and 30-Percent-Chord Trailing-Edge Flap, NASA RM L9J05, January 1950.
- 172 Czarnecki, K.R., and Mueller, J.N., Investigation at Supersonic Speeds of Some of the Factors Affecting the Flow Over a Rectangular Wing with Symmetrical Circular-Arc Section and 30-Percent-Chord Trailing-Edge Flap, NACA RM L50J13, January 1951 (Confidential).
- 173 Dunning, R.W., Ulmann, E.F., Aerodynamic Characteristics at Mach Number 4.04 of a Rectangular Wing of Aspect Ratio 1.33 Having a 6-Percent-Thick Circular-Arc Profile and a 30-Percent-Chord Full-Span Trailing-Edge Flap, NACA RM L53D03, May 1953 (Confidential).
- 174 Ridyard, H.W., and Fetterman, D.E., Aerodynamic Characteristics of a 6-Percent-Thick Symmetrical Circular-Arc Airfoil Having a 30-Percent-Chord Trailing-Edge Flap at a Mach Number of 6.9, NACA RM L56B24, June 1956.
- 175 Lord, D.R., and Czarnecki, K.R., Analysis of Pressure Distributions For a Series of Tip and Trailing-Edge Controls on a 60° Delta Wing at Mach Numbers of 1.61 and 2.01, NACA RM L58C07, May 1958.

REFERENCES (Cont.)

- 176 Czarnecki, K.R., and Lord, D.R., Span Loadings and Aerodynamic Characteristics for a Series of Tip and Trailing-Edge Controls on a 60° Delta Wing at Mach Numbers of 1.61 and 2.01, NASA TM X-51, September 1959 (Confidential).
- 177 Lord, D.R., Analysis of Pressure Distributions for a Series of Controls on a 40° Sweptback Wing at a Mach Number of 1.61, NASA TM X-139, November 1959 (Confidential).
- 178 Lord, D.R., and Czarnecki, K.R., Aerodynamic Characteristics of Several Flap-Type Trailing-Edge Controls on a Trapezoidal Wing at Mach Numbers of 1.61 and 2.01, NACA RM L54D19, June 1954.
- 179 Lord, D.R., Tabulated Pressure Data for a Series of Controls on a 40° Sweptback Wing at Mach Numbers of 1.61 and 2.01, NACA RM L57H30, November 1957, (Confidential).
- 180 Lord, D.R., and Czarnecki, K.R., Pressure Distributions and Aerodynamic Characteristics of Several Spoiler-Type Controls on a Trapezoidal Wing at Mach Numbers of 1.61 and 2.01, NACA RM L56E22, July 1956.
- 181 Lord, D.R., and Czarnecki, K.R., Aerodynamic Characteristics of a Full-Span Trailing-Edge Control on a 60° Delta Wing with and without a Spoiler at Mach Number 1.61, NACA RM L53L17, March 1954 (Confidential).
- 182 Czarnecki, K.R., and Lord, D.R., Preliminary Investigation of the Effect of Fences and Balancing Tabs on the Hinge-Moment Characteristics of a Tip Control on a 60° Delta Wing at Mach Number 1.61, NACA RM L53D14, May 1953 (Confidential).
- 183 Lord, D.R., and Czarnecki, K.R., Tabulated Pressure Data for General Flap-Type Trailing-Edge Controls on a Trapezoidal Wing at Mach Numbers of 1.61 and 2.01, NACA RM L55J04, February 1956 (Confidential).
- 184 Lord, D.R., and Czarnecki, K.R., Pressure Distribution and Aerodynamic Loadings for Several Flap-Type Trailing-Edge Controls on a Trapezoidal Wing at Mach Numbers of 1.61 and 2.01, NACA TM L55J03, March 1956.

REFERENCES (Cont.)

- 185 Lord, D.R., and Czarnecki, K.R., Tabulated Pressure Data for a Series of Controls on a 60° Delta Wing at Mach Numbers of 1.61 and 2.01, NACA RM L55L05, March 1956 (Confidential).
- 186 Lord, D.R., and Czarnecki, K.R., Hinge-Moment Characteristics for a Series of Controls and Balancing Devices on a 60° Delta Wing at Mach Numbers of 1.61 and 2.01, NACA RM L57B01, April 1957 (Confidential).
- 187 Mueller, J.N., An Investigation at Mach Number 2.40 of Flap-Type Controls Equipped with Overhang Nose Balances, NACA RM L53I21, November 1953 (Confidential).
- 188 Clark, F., and Evans, J., Some Aerodynamic and Control Studies of Lifting Reentry Configurations at Angles of Attack Up to 90° at a Mach Number of 2.91, NASA Technical Memorandum X-333, November 1960.
- 189 Foster, G.V., Exploratory Investigation at Mach Number of 2.01 of the Longitudinal Stability and Control Characteristics of a Winged Reentry Configuration, NASA TM X-173, December 1959.
- 190 Foster, G.V., Static Stability Characteristics of a Series of Hypersonic Boost-Glide Configurations at Mach Numbers of 1.41 and 2.01, NASA TM X-167, November 1959 (Confidential).
- 191 Guy, L.D., Hinge-Moment and Effectiveness Characteristics of an Aspect-Ratio-8.2 Flap-Type Control on a 60° Delta Wing at Mach Numbers from 0.72 to 1.96, NACA RM L56J17, January 1957.
- 192 Robinson, R.B., and Spearman, M.L., Aerodynamic Characteristics for Combined Angles of Attack and Sideslip of a Low-Aspect-Ratio Cruciform-Wing Missile Configuration Employing Various Canard and Trailing-Edge Flap Controls at a Mach Number of 2.01, NASA Memo 10-2-58L, October 1958.
- 193 Boyd, J.W., and Menees, G.P., Longitudinal Stability and Control Characteristics at Mach Numbers from 0.70 to 2.22 of a Triangular Wing Configuration Equipped with a Canard Control, a Trailing-Edge-Flap Control, or a Cambered Forebody, NASA Memo 4-21-59A, April 1959 (Confidential).

REFERENCES (Cont.)

- 194 Grimaud, J.E., Wind-Tunnel Investigation at a Mach Number of 2.91 of Stability and Control Characteristics of Three Lifting Reentry Configurations at Angles of Attack up to 90 Degrees, NASA TM X-455, March 1961 (Confidential).
- 195 Presnell, J.G., Investigation of the Aerodynamic and Control Characteristics of a Hypersonic Glider at Mach Numbers from 1.66 to 4.65, NASA TM X-520, June 1961.
- 196 Gloria, H.R., and Weng, T.J., Effects of Two Trailing-Edge Controls on the Aerodynamic Characteristics of a Rectangular Wing and Body at Mach Numbers from 3.00 to 5.05, NACA RM A55K07, February 1956 (Confidential).
- 197 Syverson, C.A., Gloria, H.R., and Sarabia, M.F., Aerodynamic Performance and Static Stability and Control of Flat-Top Hypersonic Gliders at Mach Numbers from 0.60 to 18, NACA RM A58G17, September 1958 (Confidential).
- 198 Ladson, C.L., and Johnston, P.J., Aerodynamic Characteristics of a Blunt-Nosed Winged Re-entry Vehicle at Supersonic and Hypersonic Speeds, NASA TM X-357, February 1961 (Confidential).
- 199 Ladson, C.L., and Johnston, P.J., Aerodynamic Characteristics of Two Winged Re-entry Vehicles at Supersonic and Hypersonic Speeds, NASA TM X-346, February 1961 (Confidential).
- 200 Rainey, R.W., Fetterman, D.E., and Smith, R., Summary of the Static Stability and Control Results of a Hypersonic Glider Investigation, NASA TM X-277, May 1960.
- 201 Clark, E.L., Kayser, L.D., Mallard, S.R., and Morris, S., Force Tests of the AD-490I-1 Dyna-Soar Models at Mach Number 8, AEDC TN 60-213, November 1960.
- 202 Close, W.H., Hypersonic Longitudinal Trim, Stability, and Control Characteristics of a Delta Wing Configuration at High Angles of Attack, NASA TM X-240, April 1960.
- 203 Rainey, R.W., Static Stability and Control of Hypersonic Gliders, NACA RM L58E12a, July 1958 (Confidential).

REFERENCES (Cont.)

- 204 Penlard, J.A., and Armstrong, W.O., Preliminary Aerodynamic Data Pertinent to Manned Satellite Re-entry Configurations, NACA RM L58E13a, July 1958.
- 205 Whitcomb, C.F., and Foss, W.E., Static Stability and Control Characteristics of Two Large Dihedral Right Triangular Pyramid Lifting Re-entry Configurations at a Mach Number of 3.05, NASA TM X-295, July 1960.
- 206 Rockhold, V.G., Onspaugh, C.M., and Marqy, W.L., Study to Determine Aerodynamic Characteristics on Hypersonic Re-entry Configurations, Part I Experimental Phase, Vol. I, Experimental Report Mach Number 2, Vol. II, Experimental Report Mach Number 5, Vol. III, Experimental Report Mach Number 8, WADD TR 61-56, January 1961.
- 207 Chauvin, L.T., Aerodynamic Heating of Aircraft Components, NACA RM L55L19b, February 1956.
- 208 Chauvin, L.T., and Buglia, J.J., Measurement of Aerodynamic Heat Transfer to a Deflected Trailing-Edge Flap on a Delta Fin in Free Flight at Mach Numbers from 1.5 to 2.6, NASA TN D-250, June 1960.
- 209 Hiers, R.S., and Hillsamer, M.E., Heat Transfer and Pressure Distribution Tests on a Blunted Delta Wing and Several Body, Elevon and Fin Attachments, AEDC TN 60-238, January 1961 (Confidential).
- 210 Peterson, V.L., and Menees, G.P., Static Stability and Control of Canard Configurations at Mach Numbers from 0.70 to 2.22 - Longitudinal Characteristics of a Triangular Wing and Unswept Canard, NACA RM A57K26, February 1958 (Confidential).
- 211 Peterson, V.L., and Boyd, J.W., Static Stability and Control of Canard Configurations at Mach Numbers from 0.70 to 2.22 - Longitudinal Characteristics of an Unswept Wing and Canard, NACA RM A57K27, February 1958.

## REFERENCES (Cont.)

- 212 Boyd, J.W., and Peterson V.L., Static Stability and Control of Canard Configurations at Mach Numbers from 0.70 to 2.22 - Longitudinal Characteristics of a Triangular Wing and Canard, NACA RM A57J15, January 1958 (Confidential).
- 213 Boyd, J.W., and Peterson, V.L., Static Stability and Control of Canard Configurations at Mach Numbers from 0.70 to 2.22 - Triangular Wing and Canard on an Extended Body, NACA RM A57K14, February 1958 (Confidential).
- 214 Spearman, M.L., and Drener, C., Effects of Forebody Length and Canard-Surface Size on the Stability and Control Characteristics of a 70° Delta-Wing Canard Airplane Configuration at a Mach Number of 2.01, NASA Memo 4-10-59L, March 1959 (Confidential).
- 215 Weng, T.J., and Gloria, H.R., Aerodynamic Characteristics of Two Rectangular-Plan-Form, All-Moveable Controls in Combination with a Slender Body of Revolution at Mach Numbers From 3.00 to 6.25, NACA RM A55J07, December 1955, (Confidential).
- 216 Metcalfe, H., Some Considerations of Shape and Control for Hypersonic Vehicles, IAS Paper No. 59-144, 1959.
- 217 Ladson, C.L., Johnston, P.J., and Trescot, C.D., Effects of Wing Plan-Form Geometry on the Aerodynamic Characteristics of a Hypersonic Glider at Mach Numbers up to 9.6, NASA TM X-286, May 1960 (Confidential).
- 218 Smith, F.M., Ulmann, E.F., and Dunning, R.W., Longitudinal and Lateral Aerodynamic Characteristics at Combined Angles of Attack and Sideslip of a Generalized Missile Model having a Rectangular Wing at a Mach Number of 4.03, NACA RM L58E26, August 1958.
- 219 Renland, J.A., Ridyard, H.W., and Fetterman, D.E., Lift, Drag and Static Longitudinal Stability Data from an Exploratory Investigation at a Mach Number of 6.86 of an Airplane Configuration having a Wing of Trapezoidal Plan-Form, NACA RM L54L03b, January 1955 (Confidential).

## REFERENCES (Cont.)

- 220 Fetterman, D.E., and Penland, J.A., Static Longitudinal Directional and Lateral Stability and Control Data from an Investigation at a Mach Number of 6.83 of Two Developmental X-15 Airplane Configurations, NASA TM X-209, March 1960 (Confidential).
- 221 Jaquet, B.M., Static Longitudinal and Lateral Stability Characteristics at a Mach Number of 3.11 of Square and Circular Plan-Form Re-entry Vehicles, with Some Effects of Controls and Leading-Edge Extensions, NASA TM X-272, May 1960 (Confidential).
- 222 Ridyard, H.W., Fetterman, D.E., and Penland, J.A., Static Lateral Stability Data from an Exploratory Investigation at a Mach Number of 6.86 of an Airplane Configuration having a Wing of Trapezoidal Plan Form, NACA RM L55A21a, February 1955 (Confidential).
- 223 Penland, J.A., Fetterman, D.E., and Ridyard, H.W., Static Longitudinal and Lateral Stability and Control Characteristics of an Airplane Configuration having a Wing of Trapezoidal Plan Form with Various Tail Airfoil Sections and Tail Arrangements at a Mach Number of 6.86, NACA RM L55F17, August 1955 (Confidential).
- 224 Ulmann, E.F., and Smith, F.M., Aerodynamic Characteristics of a 60° Delta Wing having a Half-Delta Tip Control at a Mach Number of 4.04, NACA RM L55A19, April 1955.
- 225 Fetterman, D.E., and Ridyard, H.W., The Effect of a Change in Airfoil Section on the Hinge-Moment Characteristics of a Half-Delta Tip Control with a 60° Sweep Angle at a Mach Number of 6.9, NACA RM L54H16a, October 1954.
- 226 Jacobson, C.R., Control Characteristics of Trailing-Edge Spoilers on Untapered Blunt Trailing-Edge Wings of Aspect Ratio 2.7 with 0° and 45° Sweepback at Mach Numbers of 1.41 and 1.96, NACA RM L52J28, December 1952.
- 227 Czarnecki, K.R., and Lord, D.R., Hinge-Moment Characteristics for Several Tip Controls on a 60° Sweptback Delta Wing at Mach Number 1.61, NACA RM L52K28, January 1953.

REFERENCES (Cont.)

- 228 Guy, L.D., Control Hinge-Moment and Effectiveness Characteristics of a 60° Half-Delta Tip Control on a 60° Delta Wing at Mach Numbers of 1.41 and 1.96, NACA RM L52H13, October 1952.
- 229 Morris, O.A., Control Hinge-Moment and Effectiveness Characteristics of Several Interchangeable Tip Controls on a 60° Delta Wing at Mach Numbers of 1.41, 1.62, and 1.96, NACA RM L53J08a, November 1953.
- 230 Lord, D.R., and Czarnecki, K.R., Aerodynamic Characteristics of Several Tip Controls on a 60° Delta Wing at a Mach Number of 1.61, NACA RM L54E25, August 1954.
- 231 Armstrong, W.O., Effect of Various Forebody Modifications on the Static Longitudinal Stability and Control Characteristics of a Re-entry Capsule at a Mach Number of 9.6, NASA TM X-469, April 1961 (Confidential).
- 232 Armstrong, W.O., Stainback, C.P., and McLellan, C.H., The Aerodynamic Force and Heat Transfer Characteristics of Lifting Re-entry Bodies, USAF-NASA Joint Conference, April 1960.
- 233 Mueller, J.N., Investigation of Spoilers at a Mach Number of 1.93 to Determine the Effects of Height and Chordwise Location on the Section Aerodynamic Characteristics of a Two-Dimensional Wing, NACA RM L52L31, March 1953.
- 234 Conner, W.D., and Mitchell, M.H., Effects of Spoiler on Airfoil Pressure Distribution and Effects of Size and Location of Spoilers on the Aerodynamic Characteristics of a Tapered Unswept Wing of Aspect Ratio 2.5 at a Mach Number of 1.90, NACA RM L50L20, January 1951.
- 235 Force Tests of the Boeing S-3661-1 Dyna-Soar Model at Mach Number 8, AEDC-TN-59-166, January 1960 (Secret).
- 236 Force Tests of the Boeing S-3661-1 Dyna-Soar Model at Mach Number 8, AEDC-TN-60-86, May 1960 (Secret).

## REFERENCES (Cont.)

- 237 Wiggins, L.F., and Kaattari, G.F., Supersonic Aerodynamic Characteristics of Triangular Plan-Form Models at Angles of Attack to 90°, NASA TM X-568, July 1961.
- 238 Amick, J.L., and Carvalho, G.F., Low Reynolds Number Aerodynamics of Flapped Airfoils at Supersonic Speeds, WADC TR 58-466, ASTIA AD 155854, September 1958.
- 239 Petersen, R., The Effects of Wing-Tip Loop on the Aerodynamic Characteristics of a Delta-Wing Aircraft at Supersonic Speeds. NASA Technical Memorandum X-363, May 1960.
- 240 Dennis, D.H., and Edwards, G.G., The Aerodynamic Characteristics of Some Lifting Bodies, USAF-NASA Joint Conference, April 1960.
- 241 Gunn, C.R., Heat-Transfer Measurements on the Apexes of Two 60° Sweptback Delta Wings (Panel Semiapex Angle of 30°) having 0° and 45° Dihedral at a Mach Number of 4.95, NASA TN D-550, January 1961.
- 242 Zakkay, V., and Tani, T., Theoretical and Experimental Investigation of the Laminar Heat Transfer Downstream of a Sharp Corner, PIBAL Report 708, AFOSR 1640, October 1961.
- 243 Strike, W.T., Influence of Suction on the Interaction of an Oblique Shock with a Turbulent Boundary Layer at Mach Number 3, AEDC TN 61-129, October 1961.
- 244 Ginoux, J.J., Leading Edge Effect on Separated Supersonic Flows, AFOSR-1197, (ASTIA AD 262 031), August 1961.
- 245 Brower, W.B., Leading-Edge Separation of Laminar Boundary Layers in Supersonic Flow, JAS, Vol. 28, No. 12, December 1961.
- 246 McConnell, D.G., Free Flight Observation of a Separated Turbulent Flow Including Heat Transfer up to Mach 3.5, NASA TN D-278, October 1961.
- 247 Gadd, G.E., Boundary Layer Separation in the Presence of Heat Transfer, AGARD Report 280, April 1960.

REFERENCES (Cont.)

- 248 Chung, P. M. and Viegas, J. R., Heat Transfer at the Reattachment Zone of Separated Laminar Boundary Layers, NASA TN D-1072, September 1961.
- 249 Carter, H. S. and Carr, R. E., Free-Flight Investigation of Heat Transfer to an Unswept Cylinder Subjected to an Incident Shock and Flow Interference from an Upstream Body at Mach Numbers up to 5.50, NASA TN D-988, October 1961.
- 250 Abbott, D. E. and Kline, S. J., Theoretical and Experimental Investigation of Flow over Single and Double Backward Facing Steps, Stanford University Report No. MD-5, (ASTIA AD 262-145), June 1961.
- 251 Nielsen, J. N. and Goodwin, F. K., Investigation of Hypersonic Flow Separation and its Effect on Aerodynamic Control Characteristics, Vidya Report 63, January 1962.
- 252 Chang, P. K., Separation of Flow, Jour. of the Franklin Institute, Vol. 272, No. 6, December 1961.

## APPENDIX - DATA TABLES

In order to facilitate the use of this report, the information contained in Refs. 171 through 240 is tabulated. The type of control investigated, the configuration upon which it was investigated, the test conditions, and the main information presented in each of the referenced reports are listed. An "X" in a column in the data section indicates the data that are presented in a given report. Similarly, in the configuration section, an "X" indicates the configuration upon which the listed control was investigated.

The tables provide the reader with a rapid method of determining the general type of information contained in each report or, conversely, just which reports contain the information the reader desires.

REFERENCE NUMBERS	171 172 173 174	175 176	177	178	179	180	181	182	183 184	185 186
<b>CONTROL</b>										
Flap	X	X	X	X	X	X	X		X	X
Fin										
Elevon										
Wing tip		X	X		X			X		X
Tip cone										
Canard										
Nose spike										
Nose cant										
Spoiler		X			X	X	X			X
<b>CONFIGURATION</b>										
Unswept wing	X									
Swept wing			X		X					
Delta wing		X					X	X		X
Arrow wing										
Trapezoidal wing				X		X			X	
Circular wing										
Pyramid										
Body										
Body + wing										
<b>TEST CONDITIONS</b>										
Range of $M_{\infty}$ values	1.6 6.9	1.6 2.0	1.6	1.6 2.0	1.6 2.0	1.6 2.0	1.6	1.6	1.6 2.0	1.6 2.0
Range of $\alpha$ values	0 16	0 15	-15 15	0 15	-15 15	-15 15	0 12	0 12	-15 15	0 15
Air tunnel	X	X	X	X	X	X	X	X	X	X
Helium tunnel										
Flight test										
<b>DATA</b>										
Force	X	X		X		X	X			
Hinge moment	X	X		X			X	X		X
Pressure	X	X	X		X	X	X		X	X
Heat transfer										
Flow photographs	X									

REFERENCE NUMBERS	187	188	189	190	191	192	193	194	195	196
<b>CONTROL</b>										
Flap	X	X	X	X	X	X	X	X	X	X
Fin				X		X				
Elevon										
Wing tip			X	X						
Tip cone										
Canard						X	X			
Nose spike										
Nose cant								X		
Spoiler										X
<b>CONFIGURATION</b>										
Unswept wing	X									X
Swept wing										
Delta wing		X	X	X	X	X	X	X	X	
Arrow wing										
Trapezoidal wing										
Circular wing										
Pyramid										
Body						X				
Body + wing		X	X	X		X	X	X	X	
<b>TEST CONDITIONS</b>										
Range of $M_{\infty}$ values	2.4	2.9	2.0	1.4 2.0	1 2.0	2.0	1 2.2	2.9	1.7 4.7	3.0 5.1
Range of $\alpha$ values	0 10	-4 90	0 90	-1 27	-10 10	0 29	-6 18	-3 90	-3 16	-2 12
Air tunnel	X	X	X	X	X	X	X	X	X	X
Helium tunnel										
Flight test										
<b>DATA</b>										
Force	X	X	X	X	X	X	X	X	X	X
Hinge moment	X				X					X
Pressure	X									
Heat transfer										
Flow photographs										

REFERENCE NUMBERS	197	198 199	200	201	202	203	204	205	206	207 208
<b>CONTROL</b>										
Flap	X	X	X	X	X	X	X	X	X	X
Fin	X	X							X	
Elevon										
Wing tip										
Tip cone			X			X				
Canard									X	
Nose spike										
Nose cant		X	X		X		X			
Spoiler										
<b>CONFIGURATION</b>										
Unswept wing										
Swept wing	X	X								
Delta wing			X	X	X	X	X	X	X	X
Arrow wing	X					X			X	
Trapezoidal wing										
Circular wing										
Pyramid							X	X		
Body							X			
Body + wing	X	X	X	X		X			X	
<b>TEST CONDITIONS</b>										
Range of $M_{\infty}$ values	1 18	1.6 9.6	6.7 18	8.1	6.7	6.9	6.9	3.1	2 22	1.5 2.6
Range of $\alpha$ values	0 12	-5 25	-3 12	-25 50	27 56	0 12	0 30	-4 24	-5 30	0 6
Air tunnel	X	X	X	X	X	X	X	X	X	
Helium tunnel	X		X							
Flight test										X
<b>DATA</b>										
Force	X	X	X	X	X	X	X	X	X	
Hinge moment										
Pressure										
Heat transfer										X
Flow photographs										

REFERENCE NUMBERS	209	210 211 212 213	214	215	217	218	219 220 222 223	221	224 225	
<b>CONTROL</b>										
Flap	X						X			
Fin	X			X	X	X	X	X		
Elevon										
Wing tip									X	
Tip cone								X		
Canard		X	X							
Nose spike										
Nose cant					X					
Spoiler										
<b>CONFIGURATION</b>										
Unswpt wing						X		X		
swept wing										
Delta wing	X	X	X		X				X	
Arrow wing										
Trapezoidal wing		X					X			
Circular wing								X		
Pyramid										
Body		X		X		X	X			
Body + wing	X	X	X		X	X	X	X		
<b>TEST CONDITIONS</b>										
Range of $M_{\infty}$ values	8	1 2.2	2.0	3.0 6.3	1 18	4.1	6.9	3.1	4.0 6.9	
Range of $\alpha$ values	-20 30	-6 18	0 20	-2 23	0 20	0 6	-5 25	-5 13	-12 12	
Air tunnel	X	X	X	X	X	X	X	X	X	
Helium tunnel					X					
Flight test										
<b>DATA</b>										
Force		X	X	X	X	X	X	X	X	
Hinge moment		X		X					X	
Pressure	X									
Heat transfer	X									
Flow photographs										

REFERENCE NUMBERS	110	168	170	231	232	237	238	239	240	
<b>CONTROL</b>										
Flap			X	X	X	X	X		X	
Fin								X		
Elevon									X	
Wing tip						X		X		
Tip cone										
Canard								X		
Nose spike				X						
Nose cant										
Spoiler										
<b>CONFIGURATION</b>										
Unswept wing							X			
Swept wing							X			
Delta wing	X	X				X		X		
Arrow wing										
Trapezoidal wing										
Circular wing										
Pyramid										
Body			X	X	X				X	
Body + wing						X		X		
<b>TEST CONDITIONS</b>										
Range of $M_{\infty}$ values	6.9 10	6.8 18	5 9	10	3 18	2.9 4.8	2.0 4.5	3.0 4.0	1 6	
Range of $\alpha$ values	60 90	0 60	-17 7	-15 25	20 60	-5 90	0 60	-4 12	0 8	
Air tunnel	X	X	X		X	X	X	X	X	
Helium tunnel		X		X	X					
Flight test										
<b>DATA</b>										
Force	X			X	X	X	X	X	X	
Hinge moment							X			
Pressure	X	X	X							
Heat transfer		X	X							
Flow photographs							X			

Aeronautical Systems Division, Wright-Patterson Air Force Base, Ohio  
Rept No. ASD-YDR-62-168. A REVIEW OF HYPERSONIC FLOW SEPARATION AND CONTROL CHARACTERISTICS. March 1962. 101 pages including illustrations. 252 References.

Unclassified Report  
A comprehensive review of high-speed flow separation and a review of available information pertaining to the effectiveness of aerodynamic controls for hypersonic vehicles are presented. Sufficient detail is presented to allow the report to serve as a self-contained, introductory work on separation phenomena; available sources of specific types of control data are tabulated for ready access.

( over )

1. Hypersonic Flow Separation
2. Aerodynamic Control Characteristics
3. Laminar Boundary Layer
4. Turbulent Boundary Layer
- I. Project No. 8219  
Task No. 821902  
Contract No. AF33(616)-8130
- II. Grumman Aircraft Engineering Corp., Bethpage, L.I., New York
- III.

- IV. L. G. Kaufman II et al.
- V. Avail Fr OTS
- VI. In ASTIA Collection

Aeronautical Systems Division, Wright-Patterson Air Force Base, Ohio  
Rept No. ASD-YDR-62-168. A REVIEW OF HYPERSONIC FLOW SEPARATION AND CONTROL CHARACTERISTICS. March 1962. 101 pages including illustrations. 252 References.

Unclassified Report  
A comprehensive review of high-speed flow separation and a review of available information pertaining to the effectiveness of aerodynamic controls for hypersonic vehicles are presented. Sufficient detail is presented to allow the report to serve as a self-contained, introductory work on separation phenomena; available sources of specific types of control data are tabulated for ready access.

( over )

1. Hypersonic Flow Separation
2. Aerodynamic Control Characteristics
3. Laminar Boundary Layer
4. Turbulent Boundary Layer
- I. Project No. 8219  
Task No. 821902  
Contract No. AF33(616)-8130
- II. Grumman Aircraft Engineering Corp., Bethpage, L.I., New York
- III.

- IV. L. G. Kaufman II et al.
- V. Avail Fr OTS
- VI. In ASTIA Collection